DJS Vol. 44 (2) (2022) - ISSN: 1012-5965 p. 133-154

Delta Journal of Science

Available online at **https://djs.journals.ekb.eg/**

Research Article

GEOLOGY

Petrology, Geochemistry and Mineral Chemistry of Neoproterozoic Granitoids, Wadi Zaghra, Southern Sinai, Egypt

Mohamed F. Ghoneim[1]; Mohamed Abu Anbar[1,*]; Ismail A. Thabit [1]; Zeinab M. Karkash[1]; Ahmed E. Masoud[1]

[1]Geology Department, Faculty of Science, Tanta University, Tanta, Egypt

***Corresponding author** Mohamed Abu Anbar **e-mail:** *mmanbar@Science.Tanta.edu.eg*

KEY WORDS

Geothermobarometry, Mineral Chemistry, Whole-rock chemistry, Granitoids, Wadi Zaghra, South Sinai, Egypt,

ABSTRACT

Wadi Zaghra granitoid intrusion comprises quartz diorite, granodiorite, tonalite, monzogranites, syenogranite, and alkali feldspar granites. Geochemically, Zaghra granitoid rocks are peraluminous magma and exhibit a transitional calc-alkaline to alkaline magma type affinity of I type, as well as island arc setting belonging to the volcanic arc regime. Microprobe data of amphiboles are calcic-type and have the composition of actinolite, actinolite hornblende, magnesio-hornblende, and edenite. Biotites are Mg-rich and meroxene types. Plagioclase has a composition of albite and oligoclase fields with minor andesine. According to mineral chemistry, Wadi Zaghra granitoid rocks crystallized at an average pressure of about 1.4 Kb and a temperature range of 650-700 °C.

1. Introduction

The Arabian-Nubian Shield (ANS) is characterized by the existence of metamorphosed volcano-sedimentary successions, ruptured ophiolitic complexes, gabbro-diorite-tonalite complexes, and unmetamorphosed volcanic and pyroclastic sequences that are extensively intruded by batholithic granodiorite-granite complexes (El-Ramly, 1972; Vail, 1985). The Neoproterozoic basement complex of the southern Sinai Peninsula in the northwestern sector of the ANS covers about 14,000 km^2 and is represented by gneisses, metamorphosed volcano-sedimentary assemblages, island arc metavolcanics, metagabbro-diorite, unmetamorphosed volcanics and sediments, layered ultramafics and mafics, and granitoids (e.g., Shimron, 1980; Bielski, 1982; Reymer, 1983; El-Sheshtawi, 1984; El-Metwally, 1986; El-Shafei and Kusky, 2003).

The evolution of the juvenile Nubian crust recorded two main geotectonic stages of granitoid magmatism (El-Ramly and Akaad, 1960; Hassan and Hashad, 1990; Abdel-Rahman, 1995). The first old syn-tectonic stage (750-610 Ma) is characterized by calc-alkaline quartz diorite, tonalite, trandhjemite, granodiorite, and granite intrusions (Stern and Hedge, 1985), which have been formed by partial melting of a mantle wedge with little or no crustal

contamination (Hussein et al., 1982) or in an ensimatic island arc setting (Gass, 1977; Bentor, 1985). The second younger late- to post-tectonic stage (610-550 Ma) is characterized by metaluminous to peraluminous, calc-alkaline to alkaline granodiorite, monzogranite, syenogranite, and alkaline granites, which have been formed by partial melting of the lower crust at the plate margin (Hussein et al., 1982).

The aims of the paper are to study the petrological, geochemical, and mineralogy-cal characteristics, as well as the geothermo-barometry of Wadi Zaghra granitoid rocks.

2. Geological setting and field relations

Wadi Zaghra covers an area of about 260 km^2 (Fig. 1) between longitudes: 34° 02′ 00″ - 34° 14′ 15″ E and latitudes: 28° 35′ 30″ -28° 42′ 00″ N. The rocks exposed in Wadi Zaghra, from the oldest to youngest, are metavolcano-sedimentary rocks (Zaghra Formation): late-syn tectonic granites (quartz diorites, granodiorites), Dokhan volcanics, and post-tectonic granites (monzogranites, syenogranites, and alkali feldspar granites). All these rock units are cross-cutting by faults and dykes of mafic, intermediate, and felsic composition.

The granitoid rock outcrops in Wadi Zaghra cover about 165 km^2 in the eastern, western, southern, and northeastern parts of the mapped area as scattered elongated outcrops, trending NW-SE, NE-SW, and roughly parallel to the general trends of the basement exposures of the whole area. The late-syn tectonic granitoid rocks cover about 100 km^2 and comprise the largest plutons of quartz diorites – granodiorites in the western and eastern parts of the traverse along Wadi Zaghra. They intrude metaconglomerate but are intruded by Dokhan volcanics and post-tectonic granites. The quartz diorite-granodiorites are cut by andesite and basalt dykes (Fig. 2). The quartz diorites occur as oval and elongated masses intruded in NW-SE trending with high relief (e.g., Gabal Umm Rweiss, 1500 m.a.s.l).

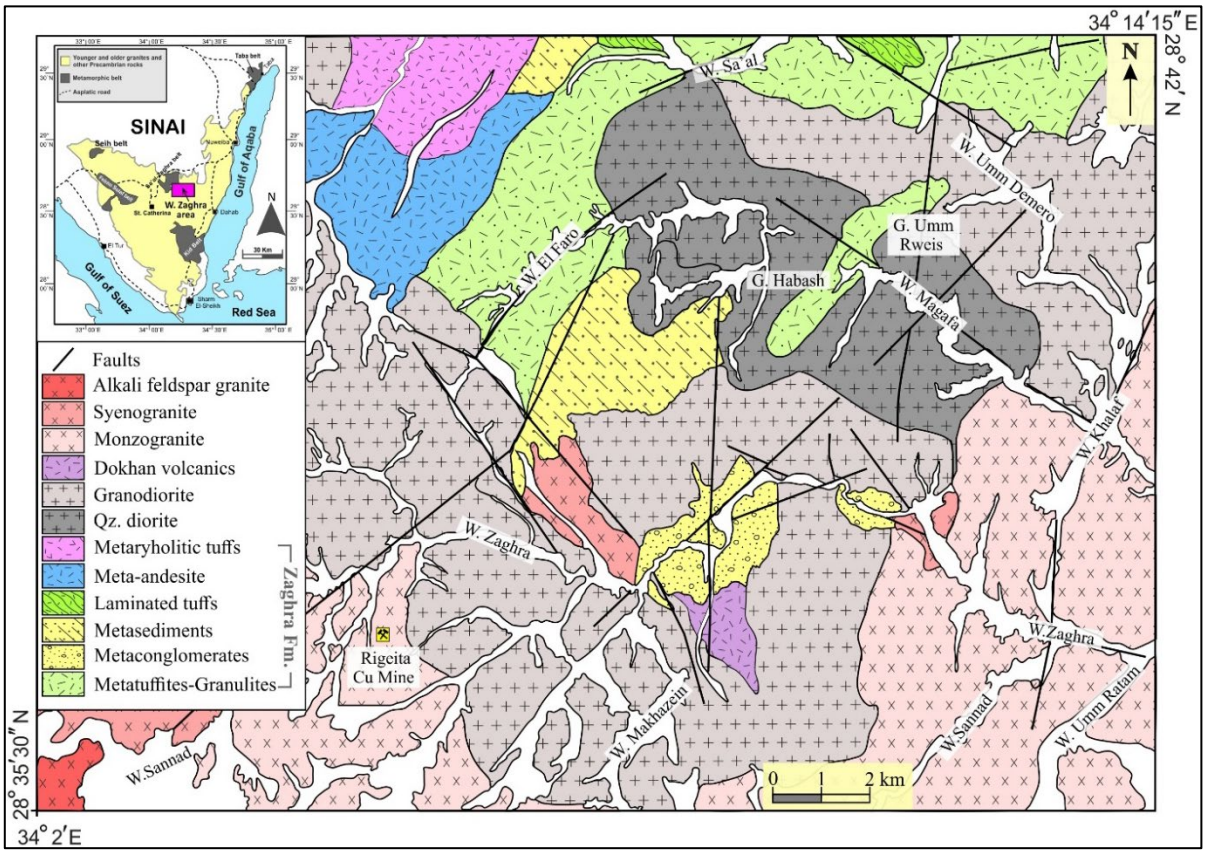

Fig. 1. Geologic Map of Wadi Zaghra area (modified after Ibrahim, 1991) with inset of geological map of southern Sinai basement complex (modified after Eyal et al., 1980).

They are intruded by the monzogranites at Wadi Magafa, as well as by small bodies of syenogranite to the east of Wadi Zaghra (Fig. 2). On the other hand, the quartz diorites are graduated into granodiorites, but they are also intruded by the monzogranites. They are coarse-grained, dark gray in color, and exhibit sharp intrusive contacts against and/or bear xenoliths of the metasediments (Fig. 2). The granodiorites occur as coarse-grained, light-gray low to moderate masses and/or apophyses, which intrude with sharp contact into and/or bear abundant xenoliths of the metavolcanic-sedimentary rocks.

The post-tectonic granitoid rocks cover an area of about 65 km^2 of monzogranite-syenogranites plutons in the mapped southwestern and southeastern parts. They enclose enclaves of granodiorites that are cut by andesitic and basaltic dykes (Fig. 2). The monzogranites occur as moderate to high elongated semi-oval masses trending NW-SE. They intrude the quartz monzodiorites but are intruded by the syenogranites as well as some basic, intermediate, and acidic dykes. The syenogranite is present as small moderate to high elongated masses cutting through the quartz diorite-granodiorite and the monzogranites in the southwestern, eastern, and central parts of the mapped area. This granite is cut by a few basic, intermediate, and acidic dykes.

3. Petrography

Microscopically, the Wadi Zaghra granitoid rocks are represented by tonalites, granodiorites, monzogranites, syeno-granites, and alkali feldspar granites.

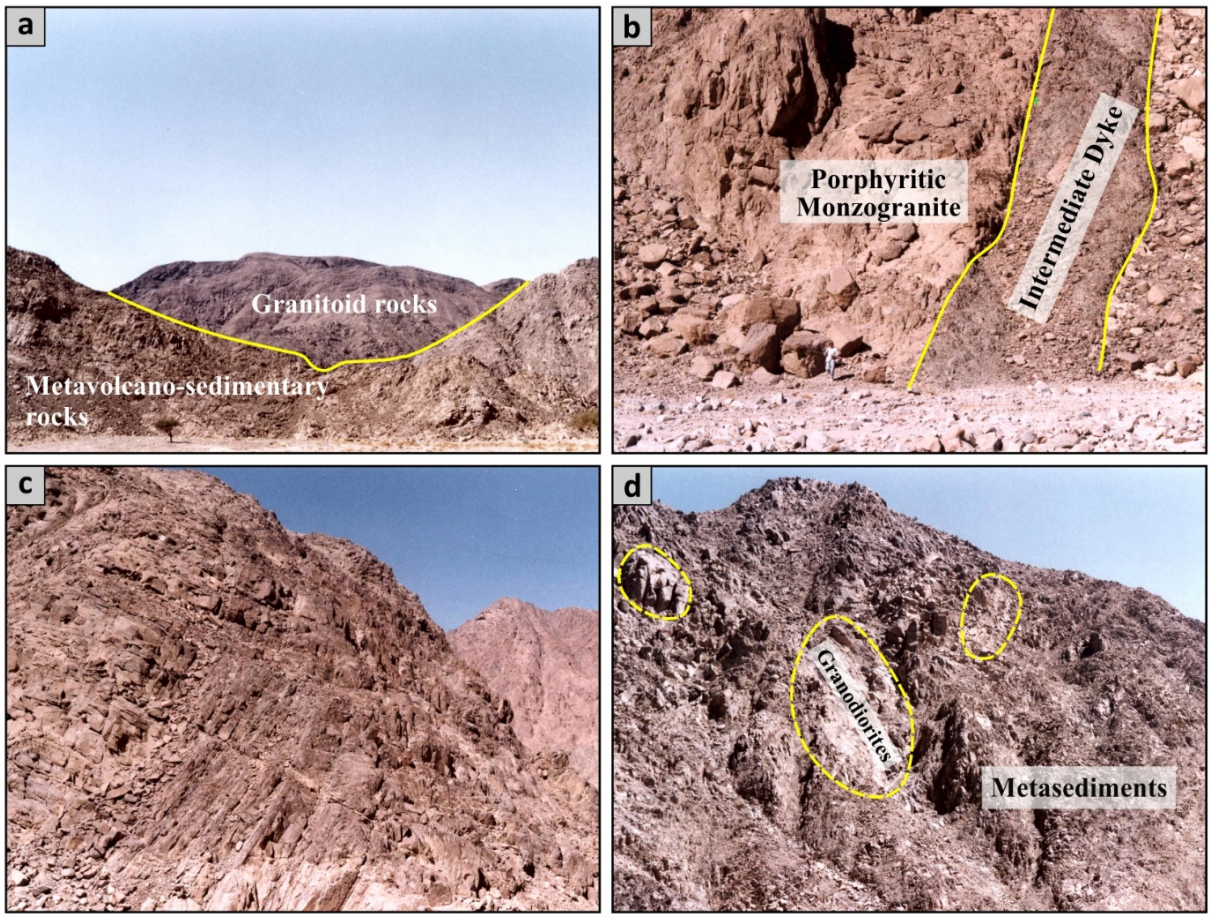

Fig. 2. (a) Granitoid rocks intruded in metavolcano-sedimentary rocks, (b) Porphyritic monzogranite dissected by andesitic dyke, (c) Inclination of metasediments, and (d) Apophyses of granodiorites in metasediments.

Quartz-diorites are medium to coarse-grained and composed of plagioclase, hornblende, and biotite with subordinate amounts of quartz. Chlorite and epidote are secondary constituents. Accessory minerals include sphene, zircon, apatite, and iron oxides. **Tonalites** are coarse-grained and consist mainly of quartz and plagioclase, with subordinate amount of biotite and hornblende (Fig. 3a). Chlorite, epidote, and sericite are secondary minerals. Apatite, zircon, iron oxide, and sphene are the main accessories. **Granodiorites** are coarse-grained and consist principally of quartz and plagioclase, with small amounts of microcline, biotite, and hornblende (Fig. 3b and c). Chlorite, epidote, and sericite are secondary minerals. Apatite, zircon, iron

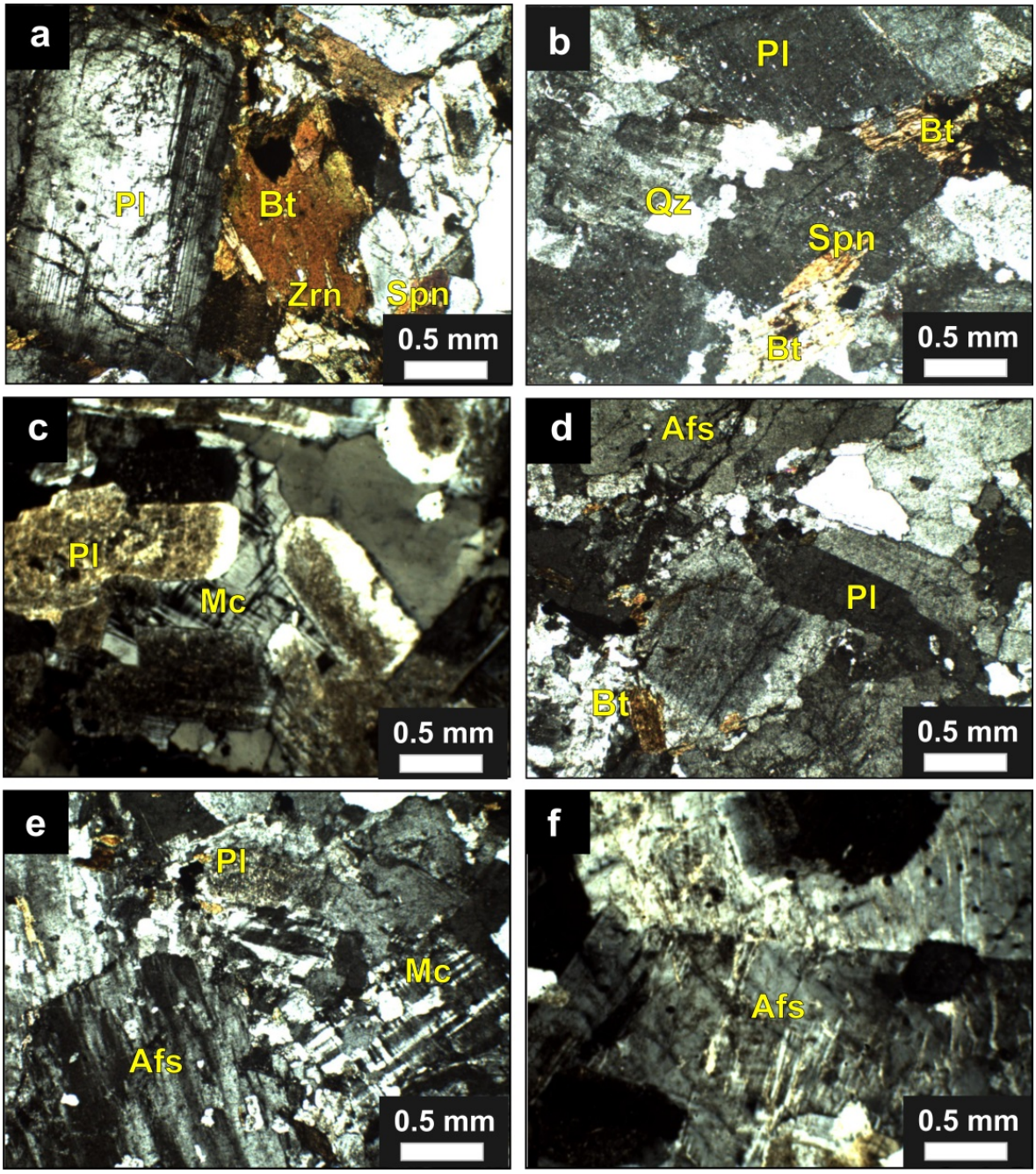

Fig. 3. Photomicrographs of (a) tonalite, (b, c) granodiorite, (d) monzogranite, (e) syenogranite, and (f) alkali feldspar granite of Wadi Zaghra granitoid rocks. coarse plagioclase showing lamellar twinning and alteration intersecting with biotite and sphene, c) potash feldspar (microcline and microperthite) intersecting by altered plagioclase crystals, d) potash feldspar as flame perthite crystals. All photomicrographs under crossed Nichols; Bt = biotite, pl = plagioclase, Qz = quartz, Mc = microcline, Afs = alkali feldspar, Spn = sphene, Zrn = zircon.

oxide, and sphene are the main accessories. **Monzogranites** are medium to coarse-grained and consist principally of quartz, plagioclase, microcline, and biotite; hornblende is uncommon (Fig. 3d). These mineral constituents often contain zircon, sphene, apatite, and iron oxides as accessory minerals, as well as chlorite, epidote, and sericite as secondary minerals. They exhibit a hypidiomorphic texture and sometimes a porphyritic texture. **Syenogranites** are medium to coarse-grained and have a pinkish-red color. They consist mainly of quartz, microcline, microcline-perthite, plagioclase, and biotite (Fig. 3e). Zircon, sphene, apatite, and iron oxides are the main accessory minerals, as well as chlorite, epidote, and sericite as secondary minerals. **Alkali feldspar granites** are characterized by granular-hypidiomorphic textures. They consist essentially of quartz, potash feldspar, and rarely plagioclase and biotite (Fig. 3f). Zircon, sphene, apatite, and iron oxides are the common accessory minerals, whereas epidote, chlorite, and sericite are secondary minerals. Quartz occurs as anhedral crystals of semicircular shape, filling the interstitial spaces between feldspar crystals. Very often, the quartz crystals enclose plagioclase, biotite, and microcline patches.

4. Analytical methodology

4.1. Whole rock analysis

Whole-rock chemical analyses for major, trace, and REE elements for 20 representative samples of Wadi Zaghra granitoid rocks were determined by using X-ray fluorescence spectrometry (XRF) at Granada University, Granada, Spain, on melt pellets in glass form using the method of Tertiani and Claisse (1982). The rock samples were crushed in a jaw crusher and ground in an electrical agate mortar to a fine powder that passed through a 100 mesh size (sieve 0.0149 mm or =15 microns). One and a half grams of the rock powder mixed well with 7.5 grams of spectromelt A19 (Di-lithium tetraborate: lithium metaborate, 66:34) to form a pellet. The mixture was then fused in a furnace for 20 minutes at 1150 °C, after which the fused bead was cooled in pellet form. Two pellets were made for each sample and examined by X-ray fluorescence in the presence of international standard samples (Abbey, 1983). As the X-ray fluorescence determines the FeO and Fe_2O_3 as total iron, the FeO is determined by the volumetric titration method using 0.1N $KMnO_4$ as well as loss on ignition (L.O.I.) (Shapiro, 1975).

4.2. Mineral analysis

Mineral analyses were carried out at the Centro de Instrumentación Científica (C.I.C.) at the University of Granada, Granada, Spain. They sorted out about 38 single-point analyses of amphiboles, biotites, and plagioclase. Mineral major-element composition was determined by wavelength-dispersive spectrometry (WDS) with a CAMECA SX-100 electron microprobe, operated at 15 kV and 15 nA, and by energy-dispersive spectrometry (EDS) with a Zeiss DSM-950 scanning microscope and a LEO 1430-VP scanning microscope, both operated at 20 kV. Natural and synthetic standards were used, and the precision was better than ±1.5% for analyzing concentrations of 10 wt.%. The electron beam was focused to a spot diameter of about 3 µm, which was occasionally raised up to -10 µm to prevent heat effects on turbed alkali feldspars and perthite. The Ziebold and Ogilive (1996) approach with the Albee and Ray (1970) ZAF correction was applied.

5. Geochemistry

5.1. Geochemical characteristics

The major element, trace elements, and rare earth elements concentrations of the studied granitoid rocks in Wadi Zaghra are listed in Table 1.

Table 1. Major Oxides (wt.%), trace elements and Rare earth elements (ppm) of the studied Zaghra granitoid rocks, South Sinai, Egypt.

Sample	Alkali feldspar granite			Syeno-monzogranite										Grano-diorite	Tonalite				Quartz-diorite	
	SA-62	SA-76	SA-91	SA-60	SA-61	SA-77	SA-78	SA-79	SA-79A	SA-93	SA-93A	SA-93B	SA-97	SA-80	SA-63G	SA-71	SA-72	SA-95	SA-92	SA-94
SiO_2	75.82	77.28	77.4	71.24	70.24	70.14	70.26	72.55	72.31	70.18	68.19	71.93	72.19	67.33	65.81	64.61	64.72	65.6	60.61	60.66
TiO_2	0.18	0.1	0.1	0.33	0.38	0.43	0.39	0.29	0.29	0.37	0.37	0.36	0.3	0.51	0.6	0.63	0.64	0.6	0.8	0.77
Al_2O_3	13.29	12.69	12.64	14.72	15.12	14.68	14.99	13.79	14.14	15.08	14.96	14.32	14.46	15.41	15.87	15.62	16.24	15.52	17.68	18.31
Fe_2O_3	0.391	0.231	0.231	0.831	0.96	1.098	0.938	0.787	0.778	0.929	1.027	0.898	0.787	1.329	1.591	1.734	1.649	1.614	2.249	2.112
FeO	0.528	0.288	0.312	1.122	1.296	1.482	1.482	1.062	1.05	1.254	1.386	1.212	1.062	1.794	2.148	2.34	2.226	2.178	3.036	2.85
MnO	0.05	0.05	0.06	0.04	0.05	0.07	0.04	0.05	0.05	0.06	0.07	0.06	0.05	0.08	0.07	0.07	0.06	0.07	0.09	0.1
MgO	0.19	0.11	0.11	0.85	1.02	1.19	1.11	0.68	0.74	0.89	0.76	0.75	0.6	1.74	2.01	2.27	2.11	2.07	2.2	1.9
CaO	0.52	0.33	0.21	1.94	2.22	0.96	1.9	1.47	1.24	1.21	1.58	0.86	1.65	3	3.39	3.55	3.82	3.72	4.08	4.6
Na_2O	4.21	4.2	4.05	4.31	4.41	4.75	4.45	3.81	3.82	4.36	5.26	4.4	4.22	4.59	4.42	4.12	4.4	4.79	4.37	4.8
K_2O	4.35	4.24	4.51	3.97	3.75	3.54	3.41	4.51	4.43	4.31	4.34	4.2	4.01	2.97	3.04	3.25	2.98	2.16	2.48	2.13
P_2O_5	0.02	0.03	0.03	0.11	0.13	0.13	0.13	0.08	0.07	0.11	0.1	0.1	0.09	0.18	0.22	0.23	0.23	0.23	0.29	0.32
LOI	0.18	0.36	0.36	0.69	0.26	1.3	1	0.52	0.76	1	0.91	0.91	0.44	0.59	0.59	0.77	0.69	0.65	1.67	0.66
Total	99.7	99.9	100	100.2	99.8	99.8	100.1	99.6	99.7	99.8	99	100	99.9	99.5	99.8	99.2	99.8	99.2	99.6	99.2
Trace and Rare earth elements (ppm)																				
Li	10	4.64	3.25	23.03	31.72	16.92	11.84	24.79	14.17	21.16	30.95	10.05	39.39	23.75	40.6	22.54	20.2	21.54	18.53	24.61
Rb	83.84	142.7	156.1	106.2	96.2	94.49	82.86	185.6	167.1	109.9	87.25	103.1	146.1	79.9	82.21	86.24	76.81	68.78	56.72	60.88
Cs	1.42	1.68	1.78	2.37	3.27	1.78	3.46	4.16	3.12	4.01	0.96	1.72	2.75	2.87	2.63	3.26	2.28	3.36	5.21	1.33
Be	1.92	3.18	3.49	2.63	2.52	2.43	2.83	3.71	3.93	2.58	1.13	2.83	3.22	2.43	2.4	2.42	2.14	2.15	1.95	1.93
Sr	47.65	28.83	28.5	510.8	597.1	258.8	507.7	279.7	274.1	286.2	272.5	282.4	273.9	659.2	697.5	762.3	842.4	821.3	662.4	813.9
Ba	289	318.4	321.3	781.9	1088	578.6	682.1	695.8	656.1	1065	760	711.1	501.2	721.1	786.4	1052	936.3	1038	704.5	780.3
Sc	2.69	2.48	2.89	3.74	4.87	4.89	4.02	3.78	4.41	3.78	4.94	3.78	3.6	9.56	6.79	8.5	7.87	8.58	12.47	7.77
V	7.88	2.01	2.17	35.13	46.08	35.13	40.66	28.88	29.35	32.4	27.16	28.93	24.78	69.9	79.11	89.49	88.26	92.02	102.5	80.42
Cr	93.4	87.07	121.3	84.94	151.6	92.25	99.94	90.72	79.9	65.03	72.52	79.24	62.39	71.01	169.2	223	95.27	72.82	158.7	64.61
Co	1.04	0.66	1.09	5.52	7.23	5.25	6.28	4.14	4.08	4.32	4.57	4.22	3.48	10.46	12.22	14.4	13.26	13.59	11.99	10.32
Ni	48.35	44.7	61.3	45.91	81.07	48.38	55.78	48.57	43.2	34.76	36.59	42.29	32.69	40.98	92.78	122.6	53.51	41.22	78.77	35.12
Cu	6.22	8.9	11.67	10.77	12.76	7.13	62.27	13.85	10.24	7.41	7.84	9.81	11.25	8.6	18.27	25.47	24.13	9.35	11.14	9.53
Zn	42.12	24.82	39.05	50.36	61.77	61.3	38.68	51.52	57.24	59.78	64.84	75.4	43.41	91.38	85.54	83.53	68.81	78.64	88.29	100.1
Ga	17.6	17.85	19.02	19.72	20.84	18.79	19.37	19.68	19.49	18.65	16.52	18.31	18.2	21.29	19.81	20.7	21.71	21.21	20.8	22.21
Y	22.86	8.57	9.43	9.34	12.06	18.96	11.07	29.37	29.32	18.5	19.5	21.19	12.48	16.28	11.47	11.23	11.79	11.89	20.83	16.35
Nb	8.58	14.12	13.34	6.62	7.43	11.47	7.15	15.09	14.02	10.05	10.78	10.35	9.28	8.92	6.65	6.31	6.67	6.47	7.84	6.93
Ta	0.56	1.11	1.04	0.57	0.62	1.01	0.6	1.7	1.55	0.76	0.84	0.82	0.91	0.65	0.52	0.49	0.53	0.43	0.47	0.41
Zr	163.9	65.4	62.9	140.4	188.5	227.7	145.9	167.2	162.6	221.1	230.2	227.5	178.6	133.3	166.6	177.7	175	178.8	244.6	362.3
Hf	4.8	2.79	2.66	4.52	5.99	7.09	4.55	5.67	5.65	6.43	6.85	6.68	5.85	4.28	4.89	5.42	5.2	5.66	7.01	8.76
Mo	1.78	1.61	2.18	1.66	2.74	1.95	2.08	2.05	1.82	1.36	1.33	1.49	1.37	1.63	3.05	4.1	1.86	1.08	2.85	1.18
Sn	1.2	2.05	2	1.1	1.05	1.72	1.11	2.54	2.41	1.53	1.96	1.82	1.94	1.38	0.92	0.97	0.99	1	1.49	0.94
Tl	0.37	0.67	0.72	0.49	0.47	0.44	0.38	0.88	0.76	0.51	0.42	0.47	0.69	0.4	0.39	0.52	0.38	0.4	0.28	0.26
Pb	18.57	26.81	22.91	135.1	20.47	14.26	17.63	25.25	27.89	15.79	11.95	11.9	18.16	15.1	15.02	15.35	170.9	14.9	29.97	9.13
U	0.89	1.85	1.98	3.57	2.51	3.15	3.54	5.36	5.45	2.81	1.31	1.61	3.79	2.42	3.89	2.77	2.29	2.16	1.89	0.92
Th	6.08	5.51	5.91	13.84	11.23	19.86	10.57	22.88	20.67	9.56	8.28	9.08	14.67	10.51	9.32	9.64	9.31	8.81	4.27	3.7
La	37.5	5.27	5.76	24.97	28.52	36.79	27.04	35.5	37.01	35.16	29.41	26.85	25.18	25.42	26.9	26.69	29.06	28.76	25.89	23.82
Ce	71.22	13.93	14.95	41.8	51.38	69.25	47.1	68.01	66.23	63.22	69.98	59.24	45.66	51	48.8	46.71	51.76	50.12	50.46	44.95
Pr	8.63	1.69	1.76	4.51	5.87	7.27	5.25	7.61	7.4	7.06	6.95	7.08	5.13	6.09	5.56	5.39	5.87	5.83	6.34	5.58
Nd	31.99	6.18	6.45	16.06	21.17	25.12	18.73	26.96	26.39	24.73	25.76	26.49	18.04	22.5	20.21	19.92	21.68	22.47	24.95	22.02
Sm	5.6	1.31	1.22	2.77	3.58	3.88	3.14	4.59	4.81	4.32	4.29	4.37	3.22	4.35	3.31	3.47	3.65	3.99	4.83	4.33
Eu	0.7	0.15	0.17	0.65	0.88	0.85	0.74	0.7	0.65	0.96	0.9	0.94	0.68	0.92	0.9	0.94	1.04	1.09	1.42	1.47
Gd	4.68	1.39	1.42	1.93	2.61	3.26	2.31	4.15	4.04	3.21	3.46	3.54	2.32	3	2.53	2.51	2.66	2.91	3.96	3.33
Tb	0.72	0.22	0.23	0.26	0.37	0.48	0.32	0.69	0.68	0.46	0.51	0.53	0.32	0.42	0.34	0.35	0.36	0.39	0.6	0.47
Dy	4.01	1.29	1.39	1.4	1.99	2.7	1.69	4.28	4.21	2.68	2.88	3.05	1.8	2.39	1.8	1.93	1.97	2.15	3.35	2.5
Ho	0.8	0.27	0.29	0.28	0.39	0.58	0.34	0.92	0.91	0.57	0.62	0.63	0.38	0.51	0.36	0.36	0.38	0.41	0.68	0.51
Er	2.11	0.82	0.84	0.76	1.06	1.7	0.94	2.62	2.61	1.57	1.64	1.74	1.05	1.39	1.02	0.94	0.99	1.07	1.82	1.3
Tm	0.29	0.15	0.16	0.12	0.17	0.28	0.16	0.45	0.46	0.25	0.27	0.28	0.18	0.22	0.16	0.15	0.15	0.16	0.27	0.2
Yb	1.78	1.05	1.09	0.85	1.09	1.89	1.06	3.12	3.09	1.77	1.84	1.87	1.32	1.48	0.99	0.99	1.03	1.08	1.8	1.27
Lu	0.25	0.17	0.18	0.14	0.17	0.32	0.16	0.49	0.49	0.28	0.29	0.3	0.22	0.25	0.15	0.16	0.16	0.17	0.28	0.2

The major oxides of the granitoid rocks in Wadi Zaghra display concentrations of SiO_2 (60.61-77.4 wt. %), TiO_2 (0.1-0.8 wt. %), Al_2O_3 (12.64-18.31 wt. %), Fe_2O_3 (0.21-2.25 wt. %), FeO (0.29-3.04 wt. %), Mg (0.11-2.27 wt. %), MnO (0.04-0.1 wt. %), CaO (0.21-4.6 wt. %), Na_2O (3.81-5.26 wt. %), K_2O (2.13-4.51 wt. %). The high field strength elements (HFSEs; such as Zr, Nb, Hf, Th, and Ta) show concentration ranges of (62.9-362.3), (6.47-15.09), (2.66-8.76), (3.7-22.88), (0.4-1.7), respectively. In addition, large ionic lithophile elements (LILEs; Ba, Rb, Sr, and U) show concentrations of (318.44-1065.27 ppm), (56.72-185.56 ppm), (28.5-842.41 ppm), and (0.92-5.45 ppm), respectively (Table 1). Moreover, they are characterized by relatively low total REE abundances (∑REE ranges between 33.89 and 170.28 ppm, with an average of 119.95 ppm) (Table 2).

Harker variation diagrams for Wadi Zaghra granitoids (Fig. 4) show strong to slight negative correlations between SiO_2 against Al_2O_3, Fe_2O_3, CaO, FeO, MgO, MnO, TiO_2, and P_2O_5 and strong to slight positive correlations between SiO_2 against K_2O and Na_2O (Fig. 4). Ba, Sr, Ga, Zr, Y, Hf, and Zn have negative correlations with SiO_2. However, Rb, Li, Cs, U, Th, Pb, Cr, and Ni have modest positive correlations with SiO_2. In addition, light rare earth elements (LREEs) exhibit positive correlations with SiO_2 (Fig. 4).

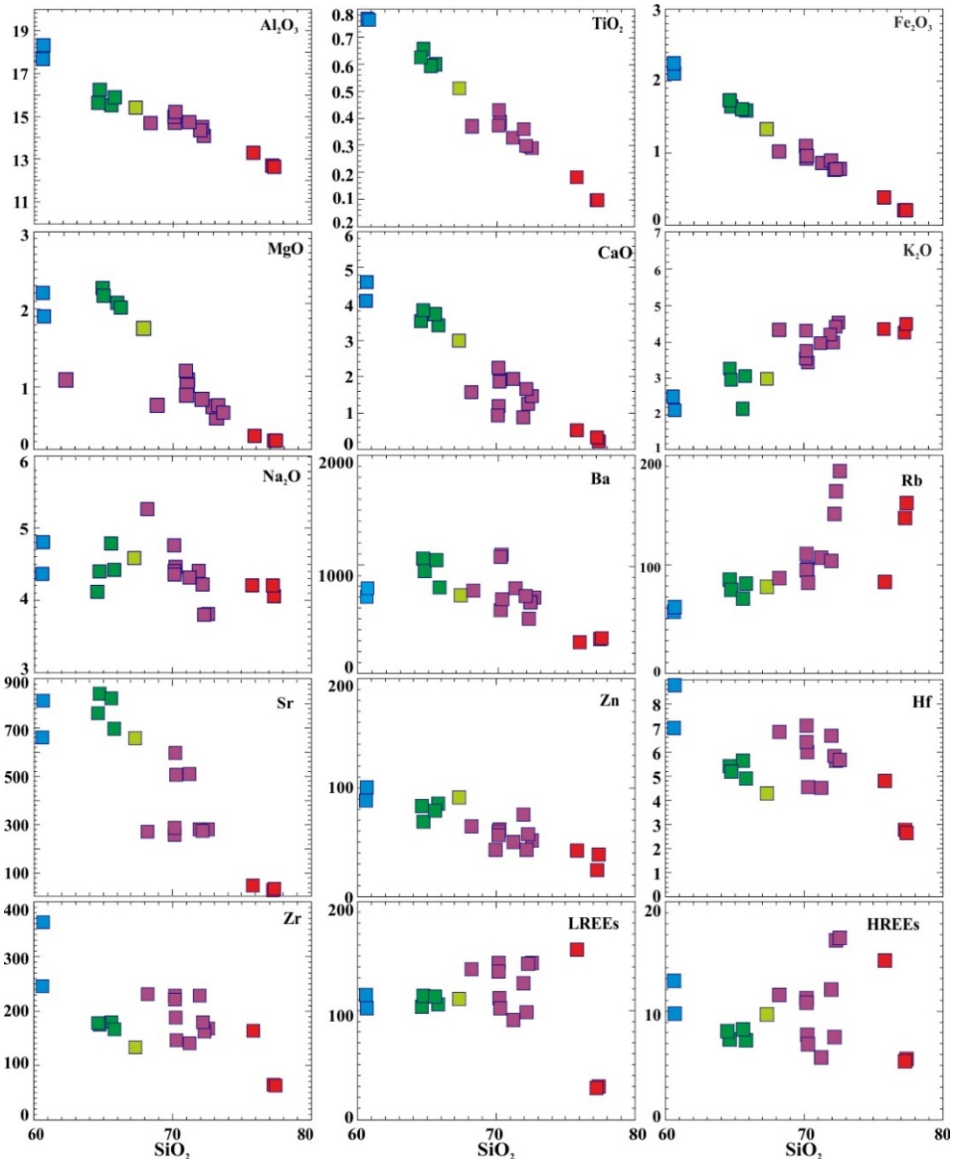

Fig. 4. Harker variation diagrams of major oxides in (wt. %), trace and REEs (ppm) versus SiO_2 (wt. %) for the studied granitoid rocks of Wadi Zaghra.

Table 2. CIPW norm and chemical ratios of the studied Zaghra granitoid rocks, South Sinai, Egypt.

Sample	Alkali feldspar granite			Syeno-monzogranite										Grano-diorite	Tonalite				Quartz-diorite	
	SA-62	SA-76	SA-91	SA-60	SA-61	SA-77	SA-78	SA-79	SA-79A	SA-93	SA-93A	SA-93B	SA-97	SA-80	SA-63G	SA-71	SA-72	SA-95	SA-92	SA-94
CIPW Norm																				
A	61.59	60.85	61.12	60.23	59.71	62.03	58.3	59.42	59.13	63.13	71.52	62.6	59.73	56.97	55.8	54.91	55.32	54.04	52.72	53.94
P	2.48	1.47	0.87	9.03	10.3	4.06	8.75	6.89	5.81	5.43	4.44	3.72	7.71	12.77	14.57	14.72	15.87	14.65	18.95	21.26
Q	33.32	35.9	36.05	25.58	23.94	25.32	25.56	29.04	29.48	24.54	17.17	27.38	27.88	20.52	18.37	17.59	16.75	19.06	13.55	11.82
C	0.74	0.65	0.77	0.03	0.03	1.58	0.8	0.12	0.95	1.28	0	1.18	0.36	0	0	0	0	0	1.01	0.42
Or	25.85	25.19	26.77	23.61	22.28	21.26	20.35	26.92	26.49	25.82	26.18	25.07	23.86	17.76	18.13	19.53	17.79	12.96	14.99	12.78
Ab	35.74	35.66	34.35	36.62	37.43	40.77	37.95	32.5	32.64	37.31	45.34	37.53	35.87	39.21	37.67	35.38	37.53	41.08	37.73	41.16
An	2.48	1.47	0.87	9.03	10.3	4.06	8.75	6.89	5.81	5.43	4.44	3.72	7.71	12.77	14.57	14.72	15.87	14.65	18.95	21.26
Di	0	0	0	0	0	0	0	0	0	0	2.41	0	0	0.97	0.88	1.45	1.53	2.18	0	0
DiWo	0	0	0	0	0	0	0	0	0	0	1.24	0	0	0.51	0.46	0.76	0.8	1.14	0	0
DiEn	0	0	0	0	0	0	0	0	0	0	0.72	0	0	0.35	0.31	0.52	0.55	0.77	0	0
DiFs	0	0	0	0	0	0	0	0	0	0	0.46	0	0	0.12	0.11	0.18	0.18	0.27	0	0
Hy	0.92	0.54	0.61	3.04	3.62	4.27	4.19	2.64	2.78	3.3	2	2.9	2.41	5.45	6.42	7.05	6.38	6.03	8.23	7.25
HyEn	0.48	0.28	0.28	2.14	2.56	3.02	2.8	1.72	1.87	2.25	1.22	1.89	1.51	4.05	4.75	5.25	4.78	4.48	5.62	4.82
HyFs	0.44	0.27	0.33	0.91	1.05	1.25	1.39	0.92	0.91	1.05	0.78	1.01	0.9	1.4	1.67	1.8	1.61	1.56	2.61	2.43
Mt	0.57	0.34	0.34	1.21	1.4	1.62	1.37	1.15	1.14	1.36	1.52	1.31	1.15	1.95	2.33	2.55	2.41	2.37	3.33	3.11
Il	0.34	0.19	0.19	0.63	0.73	0.83	0.75	0.56	0.56	0.71	0.72	0.69	0.57	0.98	1.15	1.22	1.23	1.16	1.55	1.48
Ap	0.04	0.07	0.07	0.24	0.29	0.29	0.29	0.18	0.15	0.24	0.22	0.22	0.2	0.4	0.48	0.51	0.51	0.51	0.65	0.71
Chemical ratios																				
FeOt	0.88	0.5	0.52	1.87	2.16	2.47	2.33	1.77	1.75	2.09	2.31	2.02	1.77	2.99	3.58	3.9	3.71	3.63	5.06	4.75
Fe_2O_3T	0.98	0.55	0.58	2.08	2.4	2.74	2.58	1.97	1.94	2.32	2.57	2.24	1.97	3.32	3.98	4.33	4.12	4.03	5.62	5.28
ACNK	1.46	1.45	1.44	1.44	1.46	1.59	1.54	1.41	1.49	1.53	1.34	1.51	1.46	1.46	1.46	1.43	1.45	1.45	1.62	1.59
ANK	1.55	1.5	1.48	1.78	1.85	1.77	1.91	1.66	1.71	1.74	1.56	1.67	1.76	2.04	2.13	2.12	2.2	2.23	2.58	2.64
R.I	2.23	2.08	2.13	2.43	2.44	2.53	2.27	2.34	2.32	2.77	3.66	2.56	2.32	2.35	2.44	2.51	2.51	2.14	2.66	2.72
K/Rb	430.5	246.6	239.7	310.2	323.5	310.9	341.5	201.7	220	325.3	412.8	338	227.8	308.4	306.9	312.7	321.9	260.6	362.8	290.3
10*4Gal/Al	2.5	2.66	2.84	2.53	2.6	2.42	2.44	2.7	2.6	2.34	2.09	2.42	2.38	2.61	2.36	2.5	2.53	2.58	2.22	2.29
Log (K2O/MgO)	1.36	1.59	1.61	0.67	0.57	0.47	0.49	0.82	0.78	0.69	0.76	0.75	0.82	0.23	0.18	0.16	0.15	0.02	0.05	0.05
Rb/Sr	1.76	4.95	5.48	0.21	0.16	0.37	0.16	0.66	0.61	0.38	0.32	0.37	0.53	0.12	0.12	0.11	0.09	0.08	0.09	0.07
1/Sr	0.02	0.03	0.04	0	0	0	0	0	0	0	0	0	0	0	0	0	0	0	0	0
Rb/Ba	43.78	44.92	44.78	40.37	38.18	38.93	29.25	49.99	42.53	42.54	77.55	36.48	45.37	32.85	34.32	35.68	35.98	31.96	29.15	31.54
La/Sm	6.7	4.04	4.72	9	7.96	9.49	8.6	7.74	7.7	8.14	6.86	6.15	7.81	5.84	8.12	7.69	7.96	7.21	5.36	5.51
$(La/Yb)_N$	14.2	3.4	3.56	19.83	17.73	13.16	17.32	7.69	8.1	13.44	10.82	9.71	12.87	11.59	18.32	18.18	19.1	17.93	9.7	12.68
$(Gd/Lu)_N$	2.33	1.01	1	1.75	1.87	1.26	1.77	1.06	1.02	1.43	1.51	1.48	1.32	1.53	2.06	1.96	2.02	2.15	1.76	2.04
$(La/Lu)_N$	15.57	3.18	3.38	18.92	17.01	11.86	17.33	7.6	7.81	13.08	10.71	9.36	11.94	10.77	18.25	17.43	18.39	17.67	9.6	12.18
$(Ce/Yb)_N$	10.35	3.44	3.55	12.73	12.25	9.5	11.57	5.65	5.56	9.27	9.88	8.21	8.95	8.92	12.75	12.2	13.05	11.98	7.25	9.18
$(Gd/Yb)_N$	2.13	1.07	1.05	1.84	1.94	1.4	1.77	1.08	1.06	1.47	1.53	1.54	1.42	1.64	2.07	2.05	2.1	2.18	1.78	2.13
$(La/Sm)_N$	4.22	2.54	2.97	5.67	5.01	5.97	5.41	4.87	4.85	5.12	4.32	3.87	4.92	3.68	5.11	4.84	5.01	4.54	3.38	3.47
Eu/Eu*	0.42	0.34	0.38	0.85	0.88	0.73	0.83	0.49	0.45	0.79	0.71	0.73	0.76	0.78	0.95	0.98	1.01	0.98	0.99	1.18
ΣREEs	170.3	33.89	35.91	96.5	119.3	154.4	109	160.1	159	146.2	148.8	136.9	105.5	119.9	113	110.5	120.8	120.6	126.7	112
ΣLREEs	155.6	28.53	30.31	90.76	111.4	143.2	102	143.4	142.5	135.5	137.3	125	97.91	110.3	105.7	103.1	113.1	112.3	113.9	102.2
ΣHREEs	14.64	5.36	5.6	5.74	7.85	11.21	6.98	16.72	16.49	10.79	11.51	11.94	7.59	9.66	7.35	7.39	7.7	8.34	12.76	9.78
D.O.S	267	277	205.5	231	224	233	224	239	238.6	181.5	236.4	245.3	193.9	237.8	197	193	193	183	278.7	243.8
D.O.A	2.52	2.24	-2.05	-0.61	-0.68	3.67	1.44	-0.15	-0.15	0.77	2.98	-3.51	-3.44	2.47	-2.04	-2.63	-2.68	-0.57	2.73	2.94
F.I	94.27	96.24	71.59	81.02	78.61	89.62	80.53	84.98	84.98	62.67	87.75	85.87	65.14	86.93	68.76	67.49	65.89	60.1	97.61	90.91
M.I	82.87	82.01	64.22	69.68	68.87	68.44	66.51	73.11	73.11	70.61	71.04	76.05	64.69	71.18	65.04	64.22	64.75	72.31	83.16	73.78
C I	1.83	1.07	1.13	4.88	5.74	6.72	6.31	4.34	4.48	5.38	6.65	4.9	4.13	9.35	10.78	12.27	11.55	11.75	13.12	11.84
D_I	94.91	96.75	97.17	85.82	83.64	87.35	83.86	88.46	88.61	87.67	88.69	89.98	87.61	77.49	74.17	72.5	72.07	73.1	66.27	65.76

5.2. Mineral chemistry

5.2.1. Amphiboles

The main objective of the present study is to estimate the variation in the chemical composition of the amphiboles to determine their nomenclature and the condition of their formation. The electron microprobe analyses for 6 single points of the amphibole minerals from Wadi Zaghra quartz-diorite and their chemical formulae based on 23 oxygen atoms and ignoring H_2O using MinPet software by Richard (1995) are listed in (Table 3).

The amphibole analyses plotted on TSi vs. Mg / (Mg + Fe) diagram (Leake, 1978) are calcic-type in composition and range from actinolite, actinolite hornblende, magnesio-hornblende, to edenite. The amphibole data on the TSi vs. CTi diagram (Leake, 1965) suggest that they are mostly of magmatic origin, with the exception of one sample (SA-94-3-2), which is shifted to the metamorphic amphibole field (Fig. 5).

Table 3. Electron microprobe analyses and structural formulae of amphiboles for quartz-diorite.

Sample	Quartz-diorite					
	SA-941		SA-943			
	1	2	1	2	3	4
SiO2	50.969	45.947	48.147	52.071	48.074	47.792
TiO2	0.644	1.394	0.902	0.364	1.545	0.829
Al2O3	4.161	6.873	5.139	3.303	6.647	4.658
Cr2O3	0	0	0	0.013	0	0
MnO	0.783	0.824	0.783	0.75	0.804	0.913
FeO	12.474	14.308	13.458	11.968	13.849	13.119
MgO	15.482	13.286	14.646	16.038	14.259	14.414
CaO	11.771	11.205	11.405	11.951	10.82	11.387
Na2O	0.671	1.413	1.094	0.495	1.461	0.845
K2O	0.336	0.545	0.496	0.196	0.458	0.423
F	0.003	0.018	0.014	0.003	0.037	0.013
Amphibole chemistry on basis of (23) oxygen atoms and ignoring of H_2O						
TSi	7.413	6.922	7.161	7.539	7.057	7.217
TAl	0.587	1.078	0.839	0.461	0.943	0.783
Sum_T	8	8	8	8	8	8
CAl	0.125	0.142	0.061	0.102	0.207	0.045
CCr	0	0	0	0.001	0	0
CFe3	0.07	0.103	0.166	0.103	0	0.221
CTi	0.07	0.158	0.101	0.04	0.171	0.094
CMg	3.357	2.984	3.248	3.462	3.121	3.245
CFe2	1.378	1.614	1.424	1.292	1.502	1.395
Sum_C	5	5	5	5	5	5
BFe2	0.069	0.086	0.084	0.054	0.198	0.041
BMn	0.096	0.105	0.099	0.092	0.1	0.117
BCa	1.834	1.809	1.818	1.854	1.702	1.842
Sum_B	2	2	2	2	2	2
ANa	0.189	0.413	0.316	0.139	0.416	0.247
AK	0.062	0.105	0.094	0.036	0.086	0.081
Sum_A	0.252	0.518	0.41	0.175	0.502	0.329
Sum_cat	15.252	15.518	15.41	15.175	15.502	15.329
CCl	0.001	0.005	0.004	0.001	0.009	0.003
Sum_oxy	23	23	23	23	23.054	23

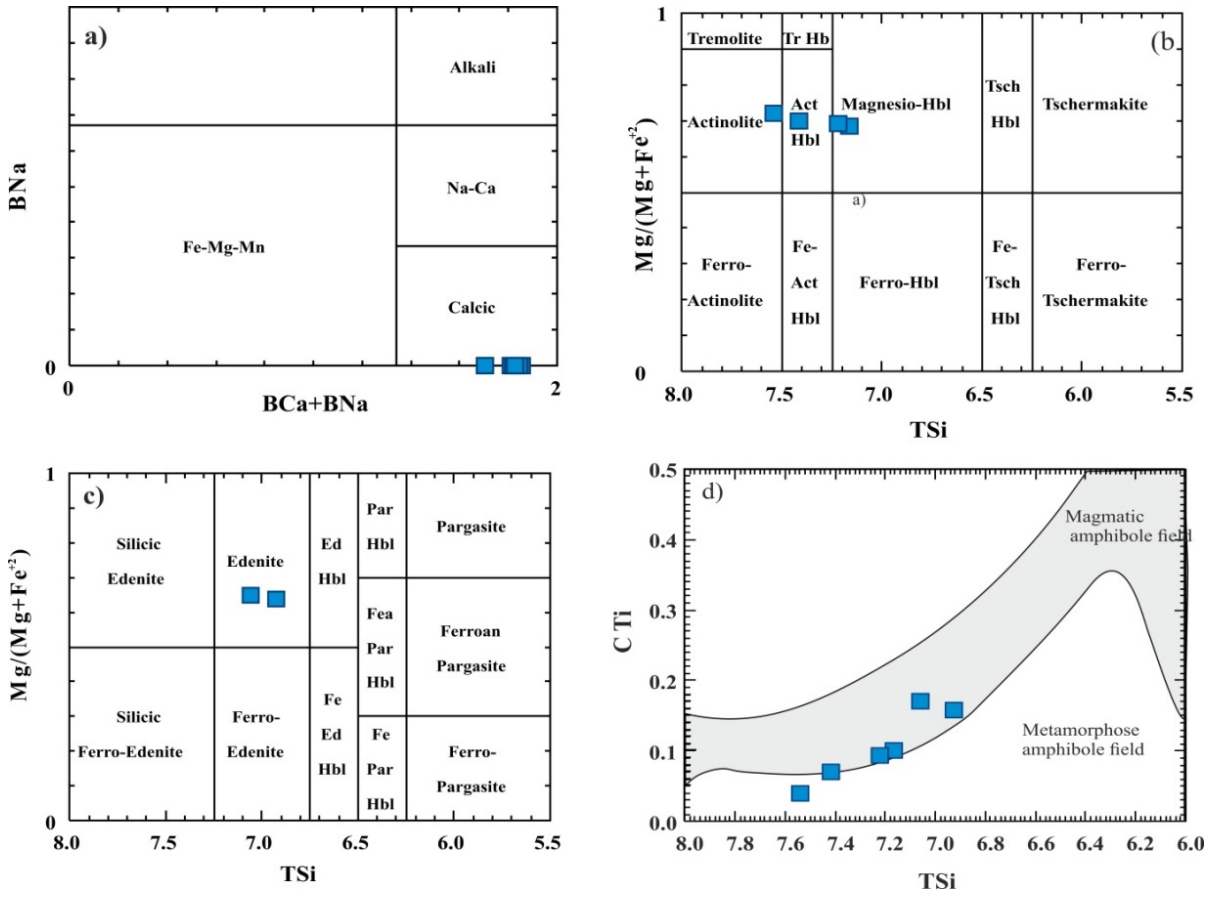

Fig. 5. Classification of amphibole of Zaghra granites, a) BNa vs. [BCa+BNa] diagram (Leake et al., 1997), (b, c) TSi vs. [Mg/ (Mg+Fe+2)] nomenclature diagram for the calcic amphibole group (Leake 1978; Leake et al., 1997), and (d) Relation between TSi vs. CTi (apfu) diagram for the studied amphiboles (Leake, 1965).

5.2.2. Biotites

Generally, the main mafic mineral in the studied granitoid rocks is biotite. A total of 14 single points microprobe analyses were performed from Wadi Zaghra syeno-monzogranite (SA-97) and quartz-diorite (SA-94). The chemical formulae were calculated (based on 24 oxygen atoms and ignoring H_2O) using Minpet software after Richard (1995). The chemical analyses and their chemical formulae are listed in (Table 4).

According to the classification of biotites by Foster (1960), all the biotites of Zaghra granitois are magnesio-biotites. Furthermore, biotites are classified as meroxene using Tröger (1969) classification diagram (Fig. 6).

5.2.3. Feldspars

Eighteen single-point analyses of feldspars from syeno-monzogranites (10 points) and quartz-diorite (8 points) have been analyzed and listed in (Table 5). The chemical formula was computed from the obtained analyses on the basis of (8) oxygen atoms using MinPet software after Richard (1995) and is listed in (Table 5).

The present feldspar data are plotted on the Or-Ab-An ternary diagram (Fig. 7) of Deer et al. (1978). The analyzed samples show that the plagioclase is plotted in the albite and oligoclase fields, except two samples from quartz-diorite lie in the andesine field, as shown in Fig. 7.

Table 4. Electron microprobe analyses and structural formulae of biotites for the studied Wadi Zaghra granitoid rocks

Sample	Quartz-diorite						Syeno-monzogranite					
	SA-941				SA-942	SA-943	SA-971			SA-972		
	1	2	3	4	1	1	1	2	3	1	2	3	4	5
SiO_2	37.06	36.6	37.05	35.29	35.86	35.87	33.74	36.79	37.46	36.42	35.69	35	36.64	36.05
TiO_2	3.586	3.555	3.399	3.633	3.957	3.384	1.269	3.503	2.543	3.601	3.596	4.187	4.263	3.642
Al_2O_3	13.82	14.07	14.01	13.57	13.85	13.76	14.96	13.29	13.52	13.07	12.77	13.13	13.74	13.48
Cr_2O_3	0.003	0.009	0.003	0.003	0.003	0.003	0.003	0.003	0.003	0.003	0.003	0.003	0.003	0.019
FeO	17.47	17.62	17.56	18.35	18.47	17.46	17.38	15.81	15.77	16.81	16.53	17.58	16.81	17.34
MnO	0.56	0.499	0.491	0.594	0.595	0.438	0.849	0.72	0.849	0.813	0.823	0.802	0.757	0.763
MgO	12.78	12.38	12.66	12.17	11.88	12.7	17.08	13.55	14.17	13.5	13.1	12.51	12.69	12.88
CaO	0.012	0.037	0.048	0.081	0.014	0.191	0.116	0.039	0.039	0.043	0.09	0.004	0.028	0.034
Na_2O	0.06	0.089	0.097	0.068	0.084	0.087	0.08	0.062	0.064	0.073	0.102	0.123	0.085	0.099
K_2O	9.428	9.375	9.452	9.123	9.416	8.424	4.266	9.41	9.123	8.969	8.906	9.186	9.187	9.315
Biotite chemistry on basis of (24) oxygen atoms and ignoring of H_2O														
Si	5.912	5.881	5.912	5.798	5.811	5.863	5.564	5.939	5.999	5.896	5.893	5.769	5.869	5.845
Al^{IV}	2.088	2.119	2.088	2.202	2.189	2.137	2.436	2.061	2.001	2.104	2.107	2.231	2.131	2.155
Al^{VI}	0.508	0.543	0.544	0.423	0.454	0.511	0.469	0.465	0.549	0.387	0.376	0.317	0.461	0.418
Ti	0.43	0.43	0.408	0.449	0.482	0.416	0.157	0.425	0.306	0.439	0.447	0.519	0.514	0.444
Fe^{2+}	2.331	2.368	2.344	2.521	2.503	2.386	2.397	2.134	2.112	2.276	2.282	2.424	2.252	2.352
Mn	0.076	0.068	0.066	0.083	0.082	0.061	0.119	0.098	0.115	0.111	0.115	0.112	0.103	0.105
Mg	3.039	2.964	3.012	2.981	2.869	3.094	4.198	3.261	3.383	3.257	3.224	3.074	3.031	3.112
Ca	0.002	0.006	0.008	0.014	0.002	0.033	0.02	0.007	0.007	0.007	0.016	0.001	0.005	0.006
Na	0.019	0.028	0.03	0.022	0.026	0.028	0.026	0.019	0.02	0.023	0.033	0.039	0.026	0.031
K	1.919	1.922	1.924	1.912	1.947	1.756	0.897	1.938	1.864	1.853	1.876	1.932	1.877	1.927
Cations	16.32	16.33	16.34	16.41	16.37	16.29	16.28	16.35	16.36	16.35	16.37	16.42	16.27	16.4
Fe#	0.43	0.44	0.44	0.46	0.47	0.44	0.36	0.4	0.38	0.41	0.41	0.44	0.43	0.43
Mg#	0.57	0.56	0.56	0.54	0.53	0.56	0.64	0.6	0.62	0.59	0.59	0.56	0.57	0.57

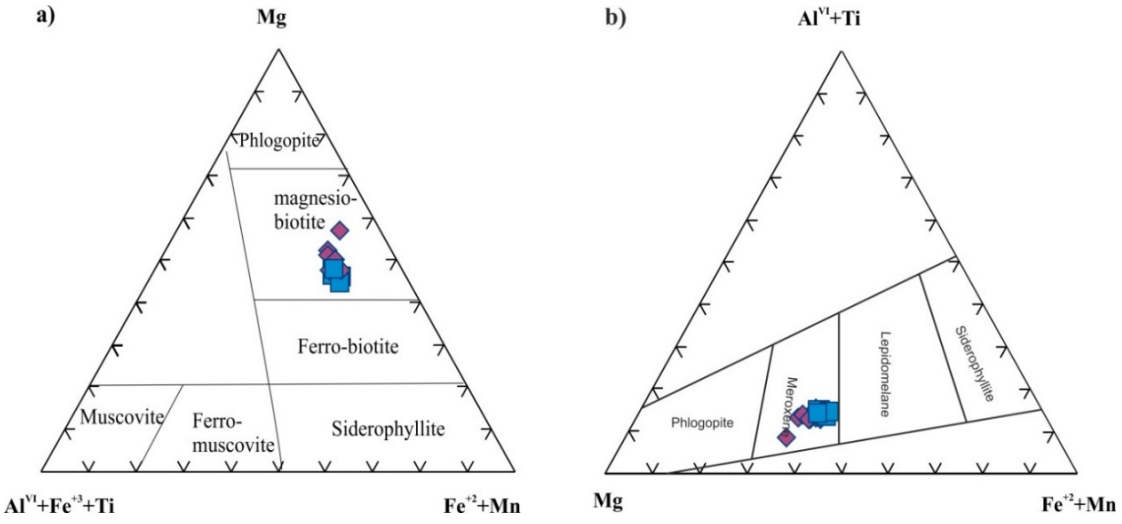

Fig. 6. (a) Classification of biotites by Foster (1960), (b) [(Al^{VI}+Ti) - Mg - (Fe^{+2}+Mn)] classification and nomenclature triangular diagram for the analyzed biotite (Tröger, 1969).

Table 5. Electron microprobe analyses and structural formulae of feldspars for the studied Wadi Zaghra granitoid rocks

	Quartz-diorite								Syeno-monzogranite									
Sample	SA-941		SA-942		SA-943				SA-971				SA-972			SA-973		
	1	2	1	2	1	2	3	4	1	2	3	4	1	2	3	1	2	3
SiO_2	60.14	62.2	55.91	63.39	65.66	59.74	59.1	63.42	62.58	65.06	65.34	76.17	66.08	65.86	61.76	65.542	63.358	65.145
TiO_2	0.011	0.019	0.011	0.001.	0.004	0.023	0.001	0.008	0.004	0.012	0	0.016	0.004	0	0	0.004	0	0.008
Al_2O_3	23.64	22.53	25.72	21.73	20.13	24.84	24.49	21.51	22.63	21.1	20.93	14.43	19.68	19.44	22.94	20.938	21.573	20.153
FeO	0.175	0.135	0.175	0.212	0.119	0.208	0.213	0.159	0.167	0.165	0.112	0.145	0.028	0.066	0.132	0.326	0.131	0.083
MnO	0.02	0.02	0.02	0.014	0.038	0.04	0.1	0.1	0.003	0	0	0	0	0	0	0.028	0	0
MgO	0.002	0.002	0.002	0.01	0.01	0.04	0.01	0.014	0	0	0.01	0	0.01	0.019	0.008	0.159	0	0.006
CaO	5.461	3.891	8.152	3.254	1.127	3.247	6.453	2.936	4.05	2.347	1.954	1.391	0.665	0.639	4.589	0.811	3.04	0.881
Na_2O	8.307	9.489	6.879	9.896	10.24	7.779	7.88	9.899	9.378	10.37	10.55	7.518	11.28	11.5	9.166	10.422	9.69	11.003
K_2O	0.491	0.161	0.234	0.324	1.571	1.585	0.205	0.389	0.272	0.301	0.228	0.107	0.103	0.059	0.177	1	0.202	0.268
Plagioclase chemistry on basis of (8) oxygen atoms																		
Si	2.726	2.798	2.585	2.838	2.931	2.72	2.68	2.85	2.798	2.886	2.9	3.261	2.958	2.959	2.774	2.909	2.852	2.931
Al	1.262	1.193	1.4	1.146	1.058	1.332	1.308	1.138	1.192	1.102	1.094	0.728	1.037	1.029	1.213	1.094	1.143	1.068
Ti	0	0	0	0	0	0	0	0	0	0	0	0	0	0	0	0	0	0
Fe^{2+}	0	0.001	0	0	0	0.001	0	0	0	0	0	0.001	0	0	0	0	0	0
Mn	0.007	0.005	0.007	0.008	0.004	0.008	0.008	0.006	0.006	0.006	0.004	0.005	0.001	0.002	0.005	0.012	0.005	0.003
Mg	0.001	0	0	0.001	0.001	0.002	0	0	0	0	0	0	0	0	0	0.001	0	0
Ca	0.265	0.188	0.404	0.156	0.054	0.158	0.314	0.141	0.194	0.112	0.093	0.064	0.032	0.031	0.221	0.039	0.147	0.042
Na	0.73	0.828	0.617	0.859	0.886	0.687	0.693	0.862	0.813	0.892	0.908	0.624	0.979	1.002	0.798	0.897	0.846	0.96
K	0.028	0.009	0.014	0.019	0.089	0.092	0.012	0.022	0.016	0.017	0.013	0.006	0.006	0.003	0.01	0.057	0.012	0.015
Cations	5.019	5.022	5.027	5.027	5.023	5.003	5.015	5.02	5.019	5.015	5.013	4.689	5.014	5.027	5.022	5.02	5.005	5.019
X	3.988	3.992	3.985	3.984	3.989	4.053	3.988	3.988	3.99	3.988	3.994	3.99	3.995	3.988	3.987	4.003	3.995	3.999
Z	1.031	1.03	1.042	1.043	1.034	0.95	1.027	1.032	1.029	1.027	1.019	0.699	1.019	1.039	1.035	1.017	1.01	1.02
Ab	71.4	80.8	59.6	83.1	86.1	73.3	68	84.1	79.5	87.4	89.5	89.9	96.3	96.7	77.6	90.3	84.2	94.4
An	25.9	18.3	39	15.1	5.2	16.9	30.8	13.8	19	11	9.2	9.2	3.1	3	21.5	3.9	14.6	4.1
Or	2.7	0.9	1.4	1.8	8.6	9.8	1.2	2.1	1.6	1.7	1.3	0.9	0.6	0.3	1	5.7	1.2	1.5

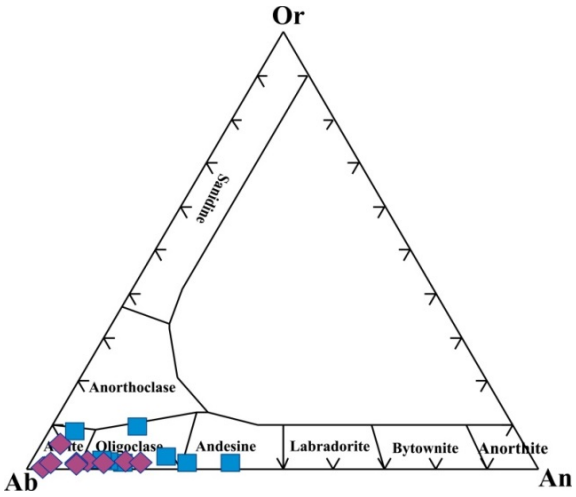

Fig. 7. Or-Ab-An ternary diagram of plagioclase composition of the studied gabbro (after Deer et al., 1978).

6. Discussion

6.1. Chemical classification

According to De la Roche et al. (1980) classification diagram, the granitoid rocks of Wadi Zaghra fall mainly within the alkali feldspar granite, syenogranite, monzo-granite, granodiorite, tonalite, and monzo-diorite fields (Fig. 8).

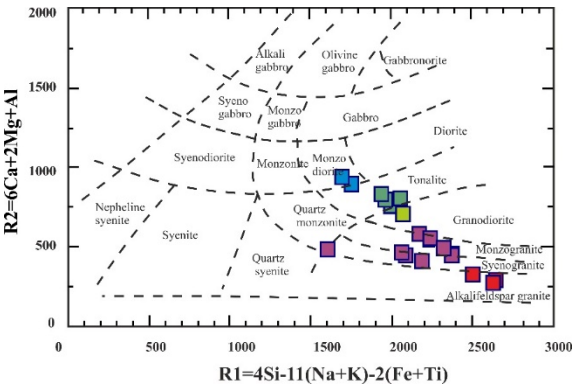

Fig. 8. R1-R2 discrimination diagram for Wadi Zaghra granitoid rocks (De La Roche et al., 1980).

6.2. Magma Type

The magma type of the Wadi Zaghra granitoids can be deduced by plotting the data on a series of diagrams. On the alkalinity ratio variation diagram of Wright (1969), quartz-diorite, granodiorite, and tonalite show calc-alkaline affinity, whereas syeno-monzogranite and alkali feldspar granite display alkaline affinity (Fig. 9a). On the agpaitic Index (AI) versus SiO_2 (wt.%) diagram of Liègeois and Black (1987), quartz-diorite, granodiorite, and tonalite belong to the calc-alkaline series, while alkali feldspar granite and sample SA-93A belong to the alkaline series (Fig. 9b).

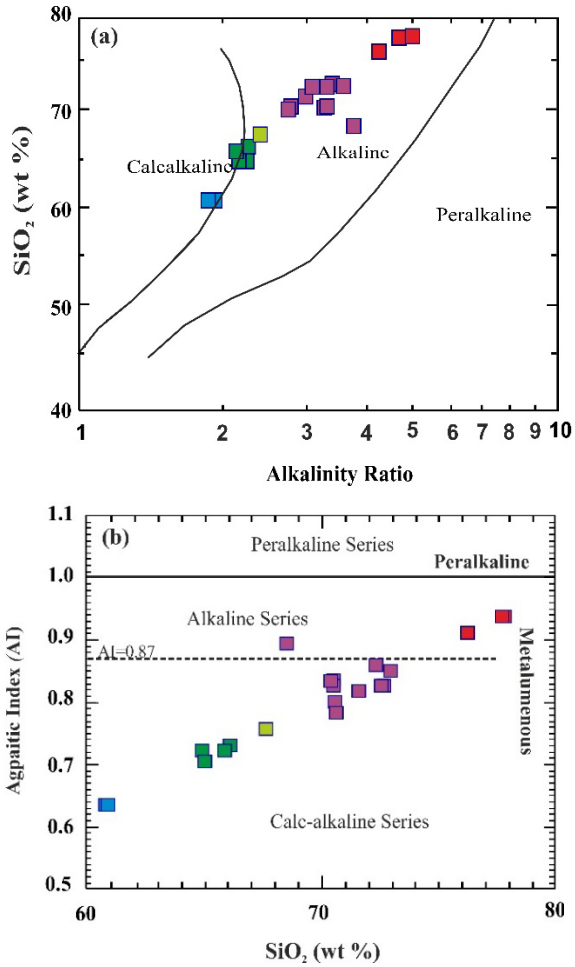

Fig. 9. (a) SiO_2 vs. Alkalinity ratio variation diagram (Wright, 1969) and (b) Agpaitic index (AI) vs. SiO_2 diagram for the study granitoids (Liègeois and Black, 1987).

The plotting on the Sylvester (1989) diagram (Fig. 10a) confirm the calc-alkaline affinity except for alkali feldspar granites, which are an alkaline + highly fractionated calc-alkaline and sample SA-93A (syeno-monzogranite) plots in the alkaline field. According to the discrimination [A/CNK (Molar $Al_2O_3/CaO+Na_2O+K_2O$) vs. A/NK (Molar Al_2O_3/Na_2O+K_2O)] diagram of Shand (1951), all Wadi Zaghra granitoids are plotted in the peraluminous field (Fig. 10b).

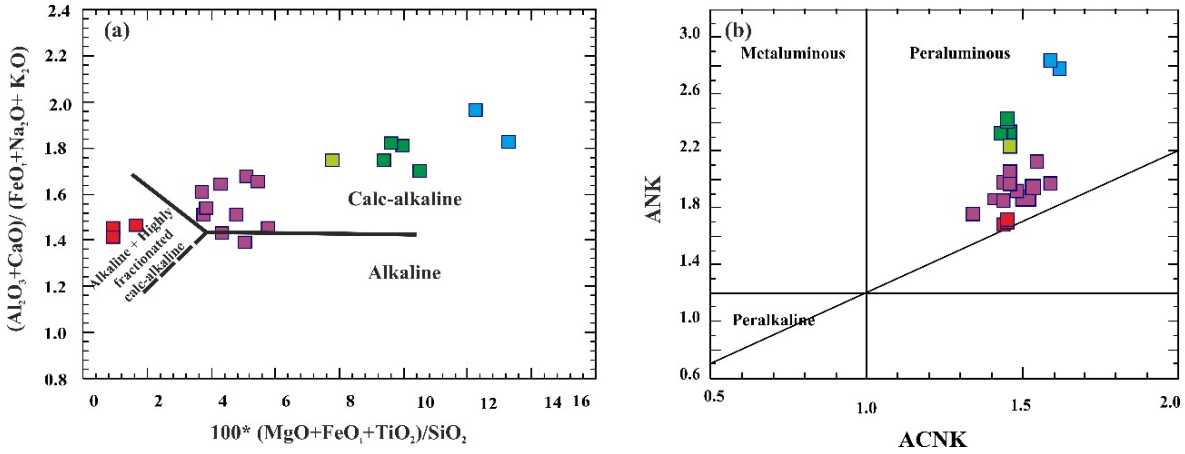

Fig. 10. (a) Plots of $(Al_2O_3+CaO)/(FeO_t+Na_2O+K_2O)$ vs. $100*(MgO+FeO_t+TiO_2)/SiO_2$ diagram (Sylvester, 1989) and (b) A/CNK vs. A/NK discrimination diagram for the studied granitoid rocks (Shand, 1951). Field boundaries are from Barker (1979) and Maniar & Piccoli (1989).

Abdel Rahman (1994) proposed FeO-MgO-Al_2O_3 triangular diagram, which is used to determine the magma type by using the biotite composition. The biotite data reflects a calc-alkaline affinity (Fig. 11).

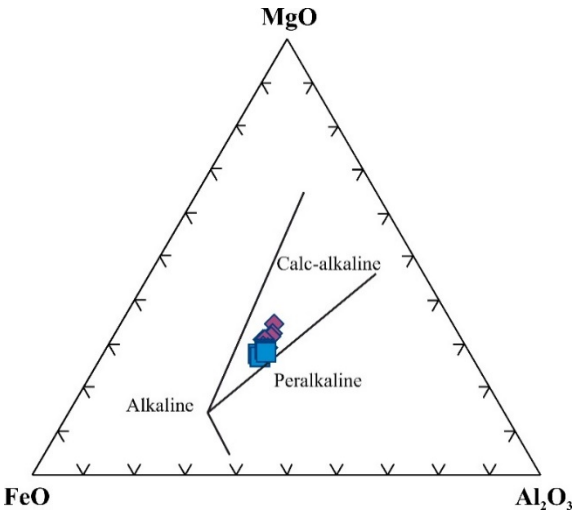

Fig. 11. Discrimination diagrams for the studied biotite (after Abdel Rahman, 1994).

6.3. Normalized multi-element diagrams and REEs patterns

The trace elements and REEs of the investigated granitoid rocks (Table 1) were normalized to chondritic values after Taylor and McLennan (1985). The spider normalized multi-element diagrams for the studied granitoid rocks (Fig. 12a) show relatively high concentrations of LILE (K, Rb, and Cs), HFSE (Zr, U, and Th), and conspicuous negative anomalies for Ni, Ti, P, Sr (samples; SA-76 and Sa-91) and Zn.

Generally, Zaghra granitoids are characterized by relatively low REE abundances (∑REE ranges between 33.89 and 170.28 ppm, with an average of 119.95 ppm). Rocks show an overall moderately fractionated chondrite-normalized REE pattern (Fig. 12b) as expressed by the chondrite-normalized $(La/Yb)_N$ ratio, varying between a most fractionated of 3.4 and the least fractionated of 19.83 (Table 2). In addition, they have $(La/Sm)_N$ ratio between 2.54 and 5.97, with an average of 4.49, whereas the $(Gd/Lu)_N$ is between 1.00 and 2.33 ppm, with an average of 1.62 ppm, indicating slight fractionation of both LREE and HREE (Table 2).

Chondrite patterns exhibit a negatively steep slope from the light to middle REEs (MREEs), and all have a gentle positive slope toward Lu (Fig. 12b). Alkali feldspar granite and syeno-monzogranite samples have negative Eu anomalies, whereas tonalite and quartz-diorite samples have no to slight positive Eu. LREEs are slightly more abundant than HREEs in terms of normalized chondrite (Fig. 12b).

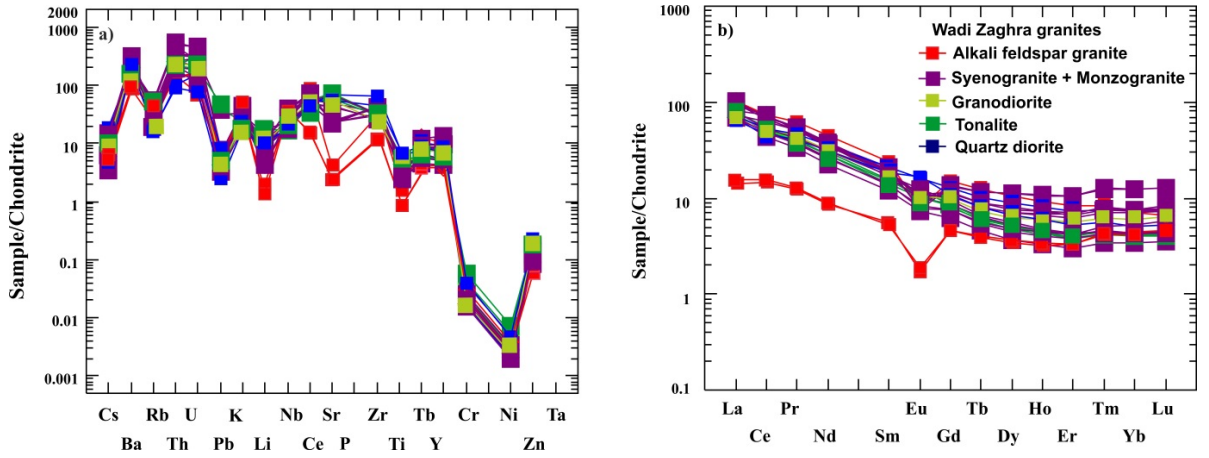

Fig. 12. (a) Normalized trace elements spider diagrams (Taylor and McLennan, 1985), (b) Normalized REE patterns for the studied granitoid rocks (Taylor and McLennan, 1985).

6.4. Tectonic setting

The Y + Nb (ppm) vs. Rb (ppm) diagram (Fig. 13) shows that Wadi Zaghra granitoid rocks lie in a volcanic arc granites field (VAG). The alkali feldspar granites and a few samples of syenogranites and monzogranites are plotted in post-orogenic granites (POG).

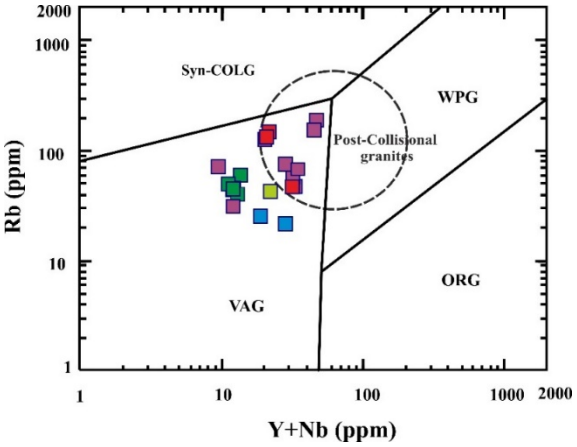

Fig. 13. Tectonic discrimination diagrams Y+Nb vs. Rb diagram, (after Pearce et al., 1984), post-collision granitoid rock dashed field (after Pearce, 1996).

Abdel-Rahman and El-Kibbi (2001) used the Rb/Sr versus K/Rb relation to distinguish between orogenic and anorogenic granitoid rocks. The plots show that Wadi Zaghra granitoid samples possess Rb/Sr ratios lower than one, indicating orogenic granitoid rocks, except alkali feldspar granites lie in anorogenic granitoid field (Fig. 14a). The SiO_2 (wt. %) vs. Nb (ppm) diagram of Kleemann and Twist (1989) shows that the Wadi Zaghra granitoid rocks plot within the I-type field of granitoid rocks (Fig. 14b).

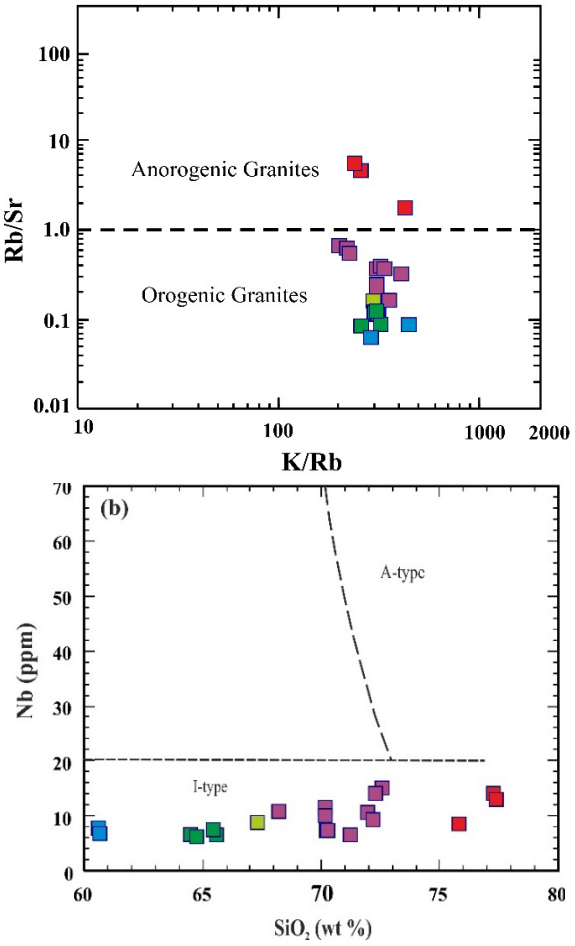

Fig. 14. (a) Rb/Sr versus K/Rb relation to discriminate between orogenic and anorogenic granitoid rocks (Abdel-Rahman and El-Kibbi, 2001), (b) I-type and A-type discrimination diagrams (Kleemann and Twist, 1989).

6.5. P-T conditions

The normative values of quartz, albite, and orthoclase for Zaghra granitoid samples are plotted on the Q-Ab-Or ternary diagram to interpret the temperatures and pressures of the granitoid rock formation (Luth et al., 1964; Winkler et al., 1975). The plot reveals that Zaghra granitoid rocks are formed at a temperature around 670 °C and pressure from 0.5 to 10 kbars, except two spots of quartz-diorite (Fig. 15a). Using the Condie (1973) discrimination diagram, the plots suggest Zaghra granitoid rocks are emplaced at a depth exceeding 30 km (Fig. 15b).

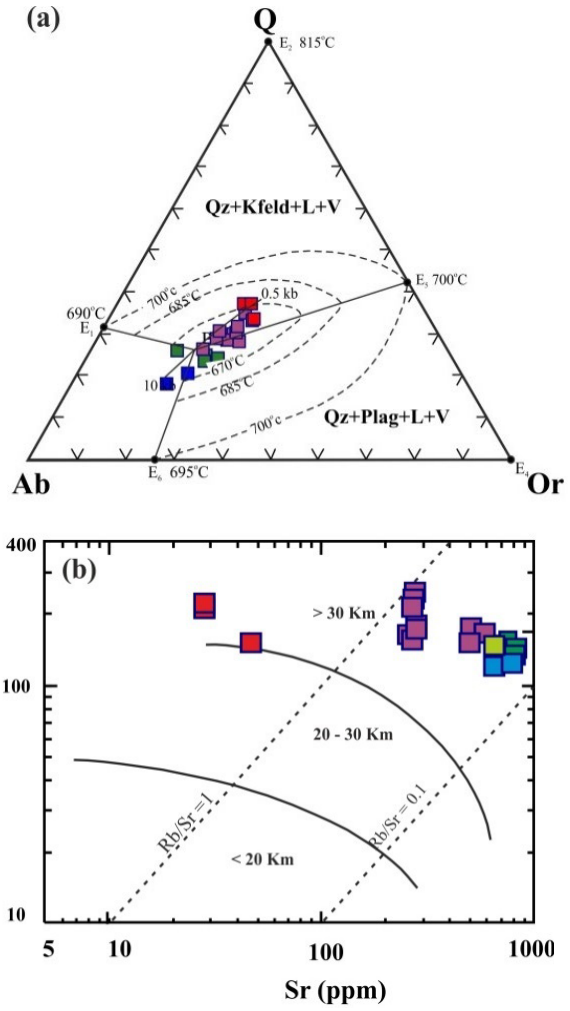

Fig. 15. (a) Q-Ab-Or system for detection temperatures and pressures of the granitoid rocks formation (Luth et al., 1964 & Winkler et al., 1975), (b) Rb (ppm) vs. Sr (ppm) variation diagram illustrating the crustal thickness during rock emplacement (after Condie, 1973).

6.5.1. Thermobarometry

It aims to determine the pressure and temperature of crystallization by using amphibole and biotite minerals.

1. Amphibole Thermobarometry

According to the relation between the Al^{IV} contents of the amphibole versus the temperature (Fig. 16a) after Blundy and Holland (1990), Wadi Zaghra granitoids record a temperature range of amphibole formation around 530-700 °C (Table 6).

In addition, depending on Hammarstrom and Zen (1986) equation ([P] (±3 Kbar) = −3.92 + 5.03 * Al^{tot}, R^2 = 0.80), the crystallization pressure of granitoid rocks from Wadi Zaghra is between 0.24 and 2.2 Kbar with an average of 1.23 Kbar, whereas according to the equation of Hollister et al., 1987 ([P] (±1 Kbar) = −4.76 + 5.64 * Al^{tot}, R^2= 0.97) the crystallization pressure is between 0.316 and 2.12 Kbar with an average of 1.39 Kbar. On the other hand, depending on Schmidt's equation (1992) ([P] (±0.6 Kbar) = −3.01 + 4.76 * Al^{tot} R^2=0.99, it is between 0.93 and 2.8 Kbar with an average of 1.87 Kbar (Table 6).

2. Biotite thermobarometry

Figure 16b shows the relation between [Ti (a.p.f.u.)] vs. [Mg/(Mg+Fe^{+2})] by Henry et al., 2005. The temperature of biotite formation in Wadi Zaghra granitoids ranges between 720 and 745 °C (Table 6).

The biotite geobarometer is applicable to almost all granitoid rocks. The pressure estimated using the total Al content in biotite by Uchinda et. al., 2007 was calculated by the following formula:

P (Kbar) = 3.03 × ^{T}Al − 6.53 (± 0.33)

Where ^{T}Al is the total Al in biotite on the basis of (O = 22). The pressure of Wadi Zaghra ranges from 0.99 to 2.27 Kbar, with an average of 1.36 Kb (Table 6). The calculated depth equals 3.267 to 7.49 km.

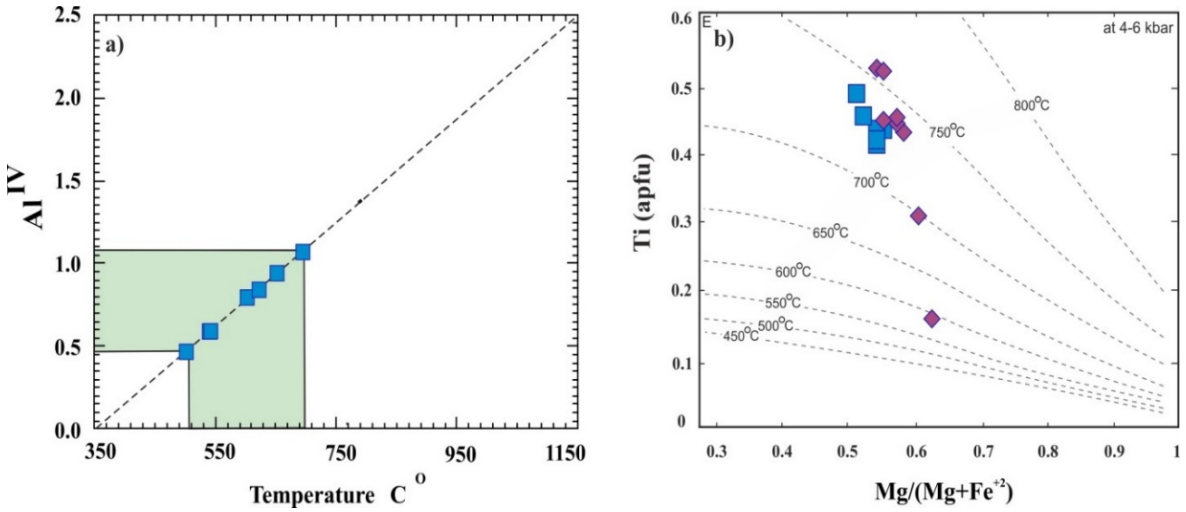

Fig. 16. (a) Al^{IV} vs. temperature standard diagram (Blundy and Holland, 1990), (b) Ti-in-biotite geothermometry (Henry et al., 2005).

Table 6. Amphiboles and biotites thermos-barometry of Wadi Zaghra granitoid rocks.

	Amphibole Barometry [P (Kbar)]			Amphibole Thermometry [T (°C)]		Biotite Thermometry [T (°C)]	Biotite Barometry [P (Kbar)]
samples	Hammarstrom &Zen, 1986	Hollister et al., 1987	Schmidt , 1992	Ridolfi & Renzulli, 2011	samples	Henry et al., 2005	Uchinda et al., 2007
					SA-941-1	728.8	1.3
SA-941-1	-	-	-	710.9	SA-941-2	726.6	1.5
					SA-941-3	719.6	1.4
SA-941-2	2.2	2.1	2.8	779.0	SA-941-4	728.2	1.4
					SA-942-1	735.6	1.5
SA-943-1	0.6	0.3	1.3	746.4	SA-943-1	722.2	1.5
					SA-971-1	587.5	2.3
SA-943-2	-	-	-	693.8	SA-971-2	734.3	1.1
					SA-971-2	694.4	1.2
SA-943-3	1.9	1.7	2.5	768.5	SA-972-1	736.1	1.0
					SA-972-2	738.4	1.0
SA-943-4	0.2	-	0.9	733.1	SA-972-3	750.8	1.2
					SA-972-4	751.7	1.3
					SA-972-5	733.0	1.3

7. Summary and Conclusion

The petrological, geochemical, and mineralogical characteristics of the studied Wadi Zaghra granitoid rocks, as well as their geologic setting and field relationships, are listed in Table 7. Generally, the granitoid rocks of Wadi Zaghra are considered to form at a temperature around 670 °C, a pressure of 0.5 to 10 kbar, and a depth of more than 30 km. According to Blundy and Holland (1990), the formation of amphibole occurs at temperatures between 530 and 700 °C, where the average pressure during crystallization is 1.4 Kbar. Additionally, the average crystallization pressure of biotite by Uchinda et al., 2007 is 1.36 Kbar, and the formation temperature of biotite by Henry et al., 2005 is 720-745 °C. The average pressure of crystallization is about 1.4 Kb, and the temperature is between 650 °C and 700 °C.

Table 7. Summary and conclusions.

	Late to syn-tectonic granitoids		Post tectonic granitoids	
Petrography	Quartz-diorite	Tonalite & Granodiorite	Syeno-monzo granites	Alkali feldspar granites
Mineralogy (Essential minerals)	plagioclase, hornblende, quartz, biotite	Quartz, plagioclase, hornblende, biotite	quartz,plagioclase, microcline microcline-perthite, biotite,	quartz, potash feldspar, less plagioclase
Magma type	Calc-alkaline & Peraluminous		Calc-alkaline to alkaline & Peraluminous	Alkaline & Peraluminous
	I-Type	I-Type	I-Type	I-Type
Tectonic setting	VAG	VAG	VAG, some are POG	VAG & POG
Orogeny	Orogenic	Orogenic	Orogenic	Anorogenic
Amphiboles	Mg-Hbl, actinolite, Hbl actinolite, edenite			
Biotites			Mg-biotite & Meroxene	
plagioclase	Oligoclase & andesine		Albite & Oligoclase	

Acknowledgments

We would like to express our sincere thanks to Prof. Fernando Bea for doing whole-rock chemistry and microprobe analyses in Granada University, Spain. Thanks to Dr. Tamer Abu-Alam, UIT the Arctic University of Norway for his constructive criticism of this manuscript. Constructive comments from two anonymous reviewers and the final revision from Prof. Yehya Abdel Gelel are highly appreciated. We wish to thank associate Editor and Editor for their editorial efforts.

References

Abbey, S., 1983. Studies in "Standard Samples" of silicate rocks and minerals, 1969-1982, Geol. Surv.Canada, Pap. 83-15.

Abdel-Rahman A. M., 1995. Tectonic–magmatic stages of shield evolution: The Pan-African belt in northeastern Egypt. Tectonophysics 242: 223–240.

Abdel-Rahman, A. F. M., 1994. Nature of biotites from alkaline, calc-alkaline and peraluminous magmas. J. Petrology, 35 (2), pp. 525-541.

Abdel-Rahman, A. M. and El-Kibbi, M. M., 2001. Anorogenic magmatism: chemical evolution of Mount El-Sibai A-type complex (Egypt): and implications for the origin of within plate felsic magmas. Geol. Mag. 138:67-85.

Barker, F., 1979. Trondhjemite: Definition, environment and hypotheses of origin: in Trondhejemites, Dacites and Related Rocks, Barker, F., Ed., Elsevier Scientific Publishing Company, pp. 1-11.

Bentor, Y.K., 1985. The crust evolution of the Arabo-Nubian Massif with special reference to the Sinai Peninsula. Precambrian Research 2, 1–74.

Bielski, M., 1982. Stages in the Arabian-Nubian Massif in Sinai (unpublished Ph.D. Thesis) - Hebrew University, Jerusalem. 155 pp.

Condie, K. C., 1973. Archean magmatism and crustal thickening. Geol. Soc. Amer. Bull., Vol. 84, pp. 2981-2991.

De La Roche, H., Letrrier, J., Granclavde, P. and Marchal, M., 1980. A classification of plutonic and volcanic rocks using R_1-R_2 diagram and major elements analyses. Its relationships with current nomenclature. Chem. Geol., 29, 183-210.

Deer, W.A., Howie, R.A. and Zussman, J., 1978: Rock-forming minerals. 2A, single chain silicates. Longman, London, 668 P.

El-Metwally, A. A. M., 1986. Mafic and ultramafic rocks north of Wadi Feiran, southern Sinai. Ph.D. Thesis, Faculty of Science, Mansoura University, Egypt, 94pp.

El-Ramly, M. F., 1972. A new geological map for the basement rocks in the Eastern and Southwestern Desert of Egypt, Scale 1:1000000. Annals of Geological Survey, Egypt,v.11, pp.1-18.

El-Ramly, M. F., and Akaad, M. K., 1960. The basement complex in the central Eastern Desert of Egypt between Latitude 24° 30′and 25° 40′ N. Geol. Surv. Egypt, Paper 8, 35 p.

El-Shafei, M.K. and Kusky, T.M., 2003. Structural and tectonic evolution of the Neoproterozoic Feiran-Solaf metamorphic belt, Sinai Peninsula: implications for the closure of the Mozambique Ocean. Precambrian Research, 123, 269-293.

El-Sheshtawi, Y. A., 1984. Petrographical and geochemical study of granitic rocks around wadi El Sheikh, South-western Sinai, Egypt. Ph. D. Thesis, Faculty of Science, Al Azhar University, Egypt, 194pp.

Eyal, M., Bartov, Y., Shimron, A. E., and Bentor, Y. K., 1980. Sinai geological map, aeromagnetic map, 1:500. 000. Geol. Soc. Ann. Meet., Ophira., Progr. Absr., p. 9.

Foster, M. D., 1960. Interpretation of the composition of trioctahedral micas. Geol. Surv. Prof. Paper., 354-B, pp. 11-49.

Gass, I. G., 1977. The evolution of the Pan African crystalline basement in NE Africa and Arabia. J. Geol. Soc. London,Vol. 134, 161p.

Hammarstrom, J. M., and Zen, E-an, 1986. Aluminum in hornblende: An empirical igneous geobarometer. Am. Mineral., 71, pp. 1297-1313.

Hassan, M. A. and Hashad, A. H., 1990. Precambrian of Egypt. In: Said, R.(Ed.): The Geology of Egypt. Balkema, Rotterdam, pp. 201–245.

Henry, D.J., Guidotti, C.V. and Thomson, J.A., 2005. The Ti-saturation surface for low to medium pressure metapelitic biotite:implications for geothermometry and Ti-substitution mechanisms. American Mineralogist, 90, 316–328.

Holland T. and Blundy J., 1994. Non-ideal interactions in calcic amphiboles and their bearing on amphibole-plagioclase thermometry, Contrib. Mineral. Petrol., 116, pp. 433-447**.**

Hollister L. S., Grisom, G. C., Peters E. K., Stowell, H. H., and Sisson, V. B., 1987. Confirmation of the empirical correlation of Al in hornblende with pressure of solidification of calc-alkaline plutons, American Mineralogist, 72, pp. 231-239.

Hussein, A.A., Ali, M.M., and El Ramly, M.F., 1982. A proposed new classification of the granites of Egypt: Journal of Volcanology and Geothermal Research, v. 14, p. 187–198.

Ibrahim, M. E., 1991. Geology and radioactivity of Wadi Zaghra area, South Central Sinai, Egypt. Ph. D. Thesis, Mansoura Univ., Egypt, 181p.

Kleemann, G. J., and Twist, D., 1989. The compositionally zoned sheet-like granite pluton of the Bushveld complex: evidence bearing on the nature of a-type magmatism. J. Petrol., 30, pp. 1383-1414. Henry, D.J., Guidotti, C.V. and Thomson, J.A. (2005) The Ti-saturation surface for low to medium pressure metapelitic bio-tite: implications for geothermometry and Ti-substitution mechanisms. American Mineralogist, 90, 316–328.

Leake, B. E., 1965. The relationship between tetrahedral aluminium and the maximum possible octahedral aluminium in natural calciferous and sub calciferous amphiboles. Am. Mineral., 50, pp. 843-854

Leake, B. E., 1978. Nomenclature of amphiboles. Can. Mineral., 16, pp. 501-520.

Leake, B. E., Woolley, A. R., Arps, C. E., Birch, W. D., Gilbert, C., Grice, J. D., Hawthorne, F. C., Kato, A., Kisch, H. J., Krivovichev, V. G., Linthout, K., Laird, J., Mandarino, J. A., Maresch, W. C., Nickel, E. H., Rock, N. M., Schumacher, J., Smith, D. C., Stephenson, N. C., Ungareth, L., Whittaker, E. J., and Youzhi, G., 1997. Nomenclature of amphiboles: Report of the subcommittee on amphiboles of the international mineralogical association, commission on new minerals and mineral names, American Mineralogist, 82, pp. 1019-1037.

Liègeois, J. P., and Black, R., 1987. Alkaline magmatism subsequent to collision in the Pan-African belt of the Adrar des Iforas (Mali). In: Fitton, J. G., Upton, B. G., (Eds.), Alkaline Igneous Rocks, Black Sci. Pub. Geol. Soc. Spec. Pub., 30, pp. 381-401.

Luth, W. C., Jahns, R. H., and Tuttle, O. F., 1964. The granite system at pressures of 4 to 10 kilobars. J. Geophys. Res., 69, pp. 759-773.

Maniar, P. D., and Piccoli, P. M., 1989. Tectonic discrimination of granitoids. Geol. Soc. Am. Bull., 101, pp. 653-643.

Pearce, J. 1996. Sources and setting granitic rocks. Episodes, 19 (4), pp. 120-125.

Pearce, J. A., Harris, N. B. W. and Tindle, A. G., 1984. Trace element discrimination diagrams for the tectonic interpretation of granitic rocks. J. Petro. 25(4) 956-983.

Reymer, A. P. S., 1983. Metamorphism and tectonics of a Pan-African terrain in southeastern Sinai. Precambrian Research 19: 225-238.

Richard, L. R., 1995. Mineralogical and Petrological data processing system. MinPet software (c), 1988-1995, version 2. 02.

Ridolfi, F., Renzulli, A., 2011. Calcic amphiboles in calc-alkaline and alkaline magmas: thermobarometric and chemometric empirical equations valid up to 1130 ºC and 2.2 GPa. Contributions to Mineralogy and Petrology, doi: 10.1007/s00410-011-0704-6.

Schmidt, M. W., 1992. Amphibole composition in tonalite as a function of pressure: an experimental calibration of the Al-in-hornblende barometer, Contrib. Mineral. Petrol., 110, 304-310.

Shand, S. J., 1951. The eruptive rocks. Wiley, New York, 356 p.

Shimron, A. E., 1980. Proterozoic island arc volcanism and sedimentation in Sinai. Precam. Res., 12, pp. 437-458.

Shimron, A.E., 1984. Evolution of the Kid Group, southeast Sinai Peninsula: thrusts, mélanges, and implications for accretionary tectonics during the Proterozoic of the Arabian-Nubian Shield. Geology 12, 242–247.

Stern, R. J., and Hedge, C. E., 1985. Geochronologic and isotopic constraints on Late Precambrian crustal evolution in the Eastern Desert of Egypt. American Journal of Science 285, 97–127.

Sylvester, P. J., 1989. Post-collisional alkaline granites. Journal of Geology, 97,:261-280.

Taylor, S. R. and McLennan, S. M., 1985. The Continental Crust. Its Composition and Evolution. Blackwell, London, p. 312.

Tertian, R., and Claisse , F., 1982. Principles of Quantitative X-ray Fluorescence Analysis

Tröger, W. E., 1969. Spezielle Petrographie der Eruptivgesteine. Ein Nomenklatur-Kompendium. mit 1. Nachtrag. Eruptivgesteinsnamen. Verlag der Deutschen Mineralogischen Gesellschaft, Stuttgart. 360 p. + 80 p.

Uchinda, E., Endo, S., Makino, M., 2007. Relationship between solidification depth of granitic rocks and formation of hydrothermal ore deposits. Resour. Geol., 57, pp. 47–56.

Vail, J. R., 1985. Pan-African (Late Precambrian) tectonic terrains and the reconstruction of the Arabian-Nubian Shield. Geology 13, 839-842.

Winkler, H., G. F, Boese, M., Marcopoules, T., 1975. Low temperature granitic melts. N. J. Mineral. Monat., 6, pp. 245-268.

Wright, J. B., 1969. A simple alkalinity ratio and its application to questions of non-orogenic granite gneiss. Geol. Mag., 106, 370-384.

Zhou, Z., 1986. The origin of intrusive mass in Fengshandong, Hubei province. Acta Petrologica Sinica. 2(I): 59-70 (in Chinese with English abstract).

Changyi, J. and Sanyuan, A., 1984. On chemical characteristics of calcic amphiboles from igneous rocks and their petrogenesis significance. Minerals and Rocks, 4(3): 1-9 (in Chinese with English abstract).

Ziebold, T.O. and Ogiliva, R.E., 1964. An empirical method for electron microprobe analysis, Anal. Chemistry, 36,322-327.

دراسة بترولوجية وجيوكيميائيــة ومعدنية علي جرانيتات البروتيروزويك العلوي في وادي زغره، جنـوب سيناء، مصــر

أ.د. محمد احمد فؤاد غنيم - أ.د. محمد أبو عنبر- زينب محمد فرج قرقش - د. إسماعيل عبدالرسول ثابت - د. أحمد السعيد إسماعيل مسعود

قسم الجيولوجيا - كليه العلوم - جامعه طنطا

الملخص

يتناول البحث الخصائص البترولوجية والجيوكيميائية والمعدنية لصخور الجرانيت في وادي زغره –جنوب سيناء بمصر، بالإضافة إلى دراسة الوضع التكتونى لهذه الصخور وعلاقتها بالصخور المجاورة. وهي عبارة عن صخور جرانيتيه تكونت أثناء وفي مرحلة متأخرة من الحركة التكتونية متمثلة في جرانوديوريت، تونالیت، كوارتز ديوريت، وصخور تكونت بعد الحركة التكتونية متمثلة في صخور المونزوجرانيت والسينوجرانيت وجرانيت الفلسبار القلوي. صخور الجرانيتات محل الدراسة وهي متداخلة في الوحدات المحيطة بها ومقطوعة بمجموعة من القواطع مافية ومتوسطة وفلسية. الدراسات البتروجرافية لهذه الصخور قد أوضحت أنها تتكون أساسا من البلاجيوكليز ومعادن الفلسبار القلوي (أرثوكلايز، الميكروكلين)، بالإضافة إلي نسب من الأمفيبول الكلسي والبيوتيت ومعادن ثانوية تشمل الكلوريت والسريسيت والابيدوت، وبعض المعادن الإضافية متمثلة في الزركون، الأباتيت، السفين، وأكاسيد الحديد. ومن الناحية الجيوكيميائية تبين أن الصهارة المكونة لصخور الجرانيت في منطقة وداي زغره تتميز بالصهارة كلسي قلوية وقلوية، قد تخارجت في بيئة جزر قوسية وأثناء تصادم الألواح وبعد الحركة الأوروجينية والارتفاع اللوحي، وتكونت عند عمق أكبر من ٣٠ كم ودرجة حرارة تتراوح بين ٦٥٠ إلى ٧٠٠ درجة مئوية في نطاق الكاتازونال والميزوزونال. أوضحت التحاليل الكيميائية أن الأمفيبول في الصخور الجرانيتية بوادي زغره عبارة عن أكتينولايت، اكتينولايت-هورنبلاند، هورنبلاند غني بالماغنيسيوم وإدينيت والبيوتيت غني بالماغنسيوم (الميروكسين)، وكل الفلسبار الموجود بها عبارة عن بلاجيوكليز من نوع الألبيت والأوليجوكليز. تكونت معادن الامفيبول عند درجات حرارة تتراوح بين ٥٣٠-٧٠٠ درجة مئوية وعند ضغط متوسطه ١,٤ كيلو بار بينما تكونت معادن البيوتيت عند درجات حرارة تتراوح بين ٧٤٥-٧٢٠ درجة مئوية وعند ضغط متوسطه ١,٣٦ كيلو بار.